nature protocols

PROTOCOL

https://doi.org/10.1038/s41596-020-0399-0

Check for updates

Proximity labeling in mammalian cells with TurboID and split-TurboID

Kelvin F. Cho[1,2,8], Tess C. Branon[3,8], Namrata D. Udeshi[4], Samuel A. Myers[4], Steven A. Carr[4] and Alice Y. Ting[2,5,6,7]✉

This protocol describes the use of TurboID and split-TurboID in proximity labeling applications for mapping protein–protein interactions and subcellular proteomes in live mammalian cells. TurboID is an engineered biotin ligase that uses ATP to convert biotin into biotin–AMP, a reactive intermediate that covalently labels proximal proteins. Optimized using directed evolution, TurboID has substantially higher activity than previously described biotin ligase–related proximity labeling methods, such as BioID, enabling higher temporal resolution and broader application in vivo. Split-TurboID consists of two inactive fragments of TurboID that can be reconstituted through protein–protein interactions or organelle–organelle interactions, which can facilitate greater targeting specificity than full-length enzymes alone. Proteins biotinylated by TurboID or split-TurboID are then enriched with streptavidin beads and identified by mass spectrometry. Here, we describe fusion construct design and characterization (variable timing), proteomic sample preparation (5–7 d), mass spectrometric data acquisition (2 d), and proteomic data analysis (1 week).

Introduction

Spatial compartmentalization evolved as a key organizing principle to regulate various molecular complexes and biological processes in living cells. The subcellular localization of a biomolecule and the molecular identities of its proximal neighbors or interacting proteins help define its biological function. Thus, a mechanistic understanding of cellular processes, whether in homeostatic or pathological states, requires elucidation of spatial patterns of localization and interactions on a system-wide level. Traditional biochemical approaches, such as subcellular fractionation and affinity purification, have contributed greatly toward this goal[1,2]. However, impurities from contaminant molecules and loss of material during these procedures greatly limit their specificity and depth of biological investigation[3,4]. Furthermore, many important subcellular regions, such as the synaptic cleft, the mitochondrial intermembrane space, various membrane-less organelles, and organellar contact sites, cannot be purified by fractionation-related approaches. Similarly, affinity purification for interactome mapping can be challenging to apply to many bait proteins, such as membrane proteins or low-abundance proteins, and transient or low-affinity protein–protein interactions are often missed.

In the past several years, a collection of alternative methods, termed proximity labeling (PL), has emerged as a complementary approach to spatial mapping at the molecular level within living cells[5]. In this protocol, we will provide an overview of PL for proteomic mapping, discuss how to determine which PL method is best suited for a given experiment, and outline how to perform subcellular proteomic mapping using the latest PL enzymes developed in our lab, TurboID[6] and split-TurboID[7].

Promiscuous labeling enzymes and their small-molecule substrates: choosing which proximity labeling method to use

Proximity labeling is carried out by enzymes that catalyze the conversion of an inert small-molecule substrate into a highly reactive and short-lived diffusible intermediate. This reactive species, which is typically conjugated to an affinity handle such as biotin, diffuses from the enzyme active site and covalently labels endogenous biomolecules in a promiscuous, but proximity-dependent manner.

[1]Cancer Biology Program, Stanford University, Stanford, CA, USA. [2]Department of Genetics, Stanford University, Stanford, CA, USA. [3]Department of Molecular and Cell Biology, University of California, Berkeley, Berkeley, CA, USA. [4]Broad Institute of MIT and Harvard, Cambridge, MA, USA. [5]Department of Biology, Stanford University, Stanford, CA, USA. [6]Department of Chemistry, Stanford University, Stanford, CA, USA. [7]Chan Zuckerberg Biohub, San Francisco, CA, USA. [8]These authors contributed equally: Kelvin F. Cho, Tess C. Branon. ✉e-mail: ayting@stanford.edu

Because the covalent tagging is performed in living cells while molecular complexes and cellular membranes are intact, the spatial relationships and interaction networks are preserved in their native state. Covalent modification provides a unique chemical handle that can then be leveraged for selective enrichment at the protein level (e.g., with streptavidin-conjugated beads) or at the peptide level (e.g., using anti-biotin antibody beads[8]) and for subsequent identification of the labeled molecules. Proximity labeling has been shown to be applicable to several classes of biological molecules, including RNA[9] and DNA[10], but PL of cellular proteins is the most well-established application. For PL of proteins, parallel advances in high-sensitivity, quantitative mass spectrometry (MS)[11–13] have provided the technological infrastructure for increasingly precise, sensitive, and unbiased spatial proteomics. A diverse set of enzymes and probes have been engineered over the past several years, each with their own strengths and caveats. Broadly, these methods can be categorized into peroxidase-related methods and biotin ligase–related methods.

Peroxidase-based proximity labeling

The 28-kDa enhanced ascorbate peroxidase (APEX/APEX2) was engineered from a plant ascorbate peroxidase (APX) by structure-guided site-directed mutagenesis and yeast-display directed evolution[14,15]. Using H_2O_2 as a co-substrate, APEX rapidly oxidizes biotin–phenol (BP) into a highly reactive phenoxyl radical that has a half-life of <1 ms[16,17] in order to tag only immediately adjacent proteins at electron-rich side chains (primarily tyrosine)[15]. Horseradish peroxidase (HRP) is larger (44 kDa or 34 kDa, with or without glycosylation, respectively) and is active only in the secretory pathway, such as within the ER lumen and at the cell surface, where the oxidizing environment permits the formation of four structurally essential disulfide bonds[18]. Although the labeling reaction mechanism is identical to that of APEX[19], HRP shows much higher catalytic activity in the secretory pathway and cell surface and is therefore ideal for PL for these applications[20]. In addition, its wide availability as an antibody conjugate makes HRP attractive for applications in fixed tissues and cells[21–23]. Although these peroxidase-based approaches have rapid labeling kinetics (<1-min labeling time required), enabling users to probe biological processes with high temporal resolution[24,25], a major limitation of these enzymes is the potential oxidative stress from the use of H_2O_2 and the low membrane permeability of BP, which make them challenging to apply in living organisms in particular.

Biotin ligase–based proximity labeling

By contrast, biotin ligase–related approaches do not require toxic reagents and instead simply utilize the highly soluble substrate biotin, while cells provide ATP (Fig. 1). However, the first versions of these enzymes have very low activity (>18 h of labeling time required)[26–28]. BioID, derived from *Escherichia coli* biotin ligase (BirA), adenylates biotin to generate a reactive intermediate, biotin–adenosine monophosphate (biotin–5′-AMP), which diffuses from its active site and reacts with lysine side chains on proximal proteins[26,29]. It has been experimentally estimated that the reactive radius of BioID-generated biotin–5′-AMP in living cells is ~10 nm[30], which is similar to the labeling radii of peroxidase-based enzymes. Additional biotin ligase–related approaches have been developed: BioID2, derived from *Aquifex aeolicus* biotin ligase, is ~30% smaller than BioID[27] and can be used at temperatures >37 °C; BASU is another promiscuous biotin ligase derived from the *Bacillus subtilis* biotin ligase[28]. Recently, a new biotin ligase–based PL method called AirID was developed using an ancestral enzyme reconstruction algorithm[31]. These enzymes all still require long labeling times (of several hours) to detect biotinylation signal[6,27,28,32–34], thereby limiting the scope of dynamic processes that can be probed.

TurboID

To overcome the slow labeling kinetics of existing biotin ligase–related methods, we utilized yeast-display directed evolution to engineer a new pair of biotin ligase PL enzymes, TurboID and mini-Turbo, with faster labeling kinetics using the same non-toxic labeling conditions that make biotin ligases ideal for in vivo applications[6]. TurboID and miniTurbo require labeling times as short as 10 min or less in cell culture, which enables probing of dynamic biological processes with much higher temporal resolution. In addition to shorter required labeling times, TurboID and miniTurbo also retain catalytic activity at lower temperatures, enabling PL in organisms such as flies, worms, yeast, and plants that are grown at <37 °C[6,35–37]. TurboID is approximately two-fold more active than miniTurbo, but miniTurbo is smaller (28 kD compared with 35 kD for TurboID). Furthermore, miniTurbo has a lower affinity for biotin, which prevents it from carrying out labeling in the absence of high concentrations of exogenous biotin, enabling tighter user control of the labeling time window.

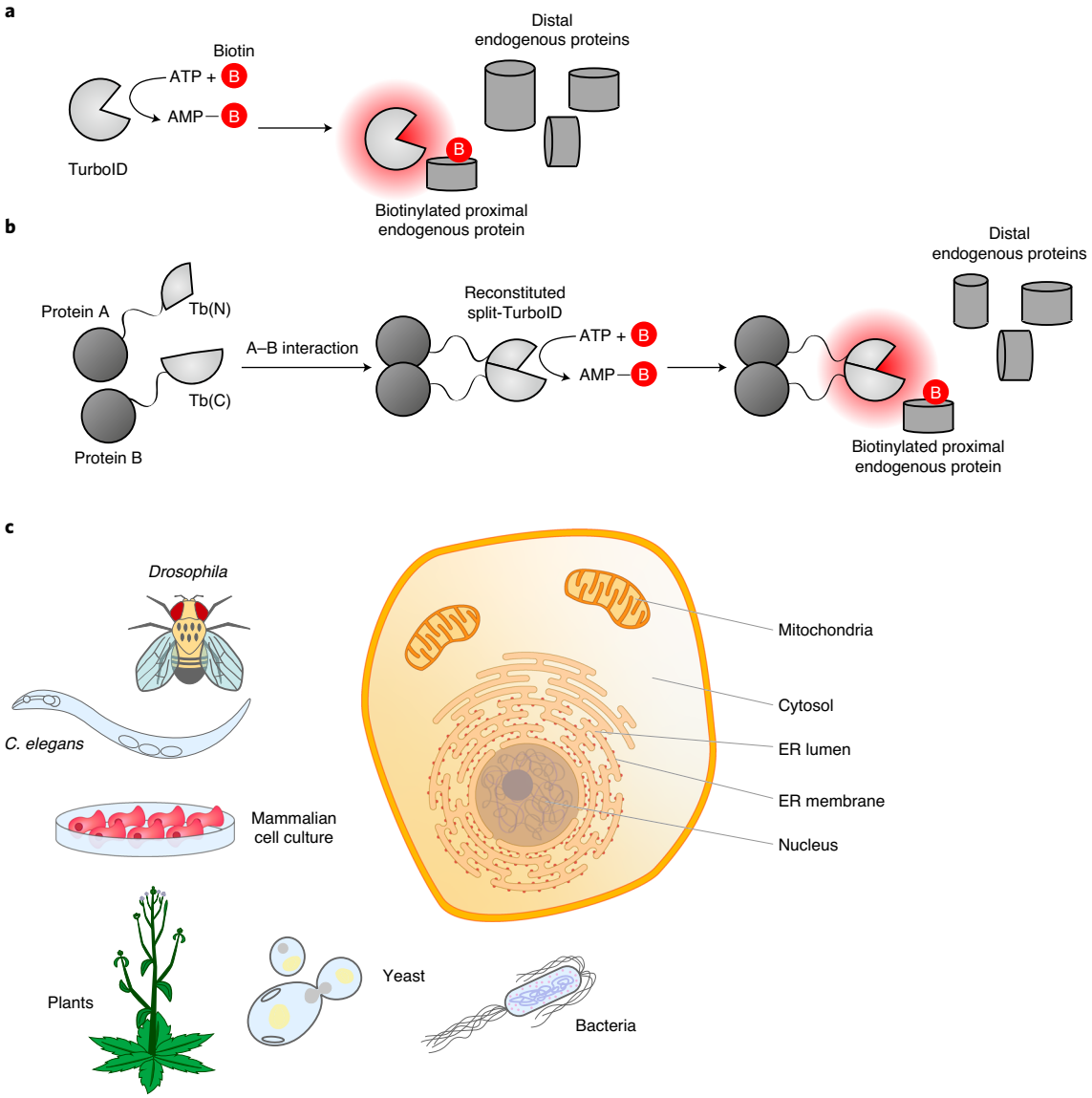

Fig. 1 | Proximity-dependent biotinylation catalyzed by TurboID and split-TurboID. a, TurboID uses ATP and biotin to generate biotin-5′-AMP, a reactive intermediate that can covalently label proximal endogenous proteins. **b**, Split-TurboID consists of two TurboID fragments (Tb(N), an N-terminal fragment, and Tb(C), a C-terminal fragment), which can be brought together by a protein–protein interaction or membrane–membrane apposition to reconstitute an active enzyme. **c**, Example model organisms and subcellular compartments in which TurboID has been used; information for other biotin ligases and PL enzymes is provided in Table 1.

Comparison of the different proximity labeling enzymes

The characteristics of the different enzymes for PL are critical factors to consider when choosing the optimal enzyme for specific types of experiments (Table 1). APEX has been widely adopted for PL experiments performed in cell culture because of its fast kinetics and high activity in nearly every cellular compartment[5,9]. APEX reagent delivery and toxicity are not typically problems in cell culture, but it requires addition of chemical quenchers to terminate the reaction. HRP has similar characteristics but can be used only in the secretory pathway or extracellularly. These peroxidase methods cannot be applied in cell types and organisms that have abundant endogenous peroxidases, such as plants, which are cross-reactive with the substrates used for PL[35,38].

Because of the difficulty of delivering peroxidase substrates to target tissues and the potential toxicity of the hydrogen peroxide required by APEX and HRP, biotin ligase–based methods are preferred for in vivo experiments. BioID has been extensively used, but it is limited by its low activity and long labeling times. BioID also has very low or undetectable activity in many model organisms, including mice, yeast, worms, flies, and plants[6,35–37,39–43], as well as in particular subcellular

Table 1 | Comparison between different proximity labeling approaches

Method	Substrates	Labeling time	Organelles demonstrated	Model organisms	Strengths	Limitations
APEX2	Biotin phenol, hydrogen peroxide	≤1 min	Cytosol, nucleus[9], nucleolus[9], mitochondrial matrix[15,77], mitochondrial intermembrane space[76], mitochondrial nucleoid[77], ER lumen[88], ERM[14,78], OMM[14,78,89], Golgi[90], autophagosome[91], cilia[92]	Mammalian cell culture, bacteria[93], yeast[14], flies[94], mice[95]	High temporal resolution and high activity in most cellular compartments; versatile and can be used for RNA labeling[9] and electron microscopy[14]	Limited application in vivo due to H_2O_2 toxicity and low BP permeability
HRP	Biotin phenol, hydrogen peroxide	≤1 min	ER lumen, cell surface[21–23], synaptic cleft[20]	Mammalian cell culture, flies[80], primary human tissue[21]	Higher activity than APEX2 in secretory pathway and extracellularly; ideal for cell surface proteomics paired with membrane impermeable BxxP substrate[80]	Limited to secretory pathway and extracellular applications; limited application in vivo due to H_2O_2 toxicity and low BP permeability
BioID	Biotin, ATP	18 h	Cytosol, nucleus[44,96], ERM[97,98], mitochondrial matrix[99], mitochondrial outer membrane[100], mitochondrial nucleoid[101], cell surface[102,103], peroxisome membrane[104], Golgi[105], cilia[56]	Mammalian cell culture, yeast[106], flies[107], plants[42], mice[40,54,73]	Non-toxic labeling conditions and extensively applied across many studies	Poor temporal resolution and limited application in vivo due to low catalytic activity
BioID2	Biotin, ATP	18 h	Cytosol, nucleus[27], ERM[108], mitochondrial intermembrane space[109], mitochondrial inner membrane[110], mitochondrial outer membrane[111], Golgi[112]	Mammalian cell culture, mice[74]	Higher activity than BioID; stable at higher temperatures	Poor temporal resolution and limited application in vivo due to low catalytic activity
BASU	Biotin, ATP	18 h	Cytosol, nucleus[28,113]	Mammalian cell culture	Higher activity than BioID	Poor temporal resolution and limited application in vivo due to low catalytic activity
AirID	Biotin, ATP	3 h	Cytosol, nucleus[31]	Mammalian cell culture	Higher activity than BioID; lower potential toxicity in long-term experiments	Poor temporal resolution and limited application in vivo due to low catalytic activity
TurboID	Biotin, ATP	≤10 min	Cytosol, nucleus, ERM, ER lumen, mitochondrial matrix, cell surface[6], OMM[7]	Mammalian cell culture, bacteria[6], yeast[6,37], flies[6], worms[6], plants[35]	Highest-activity promiscuous biotin ligase	Potentially less user control of labeling window because of high biotin affinity; potential toxicity in long-term experiments
miniTurbo	Biotin, ATP	≤10 min	Cytosol, nucleus, ERM, ER lumen, mitochondrial matrix, cell surface[6]	Mammalian cell culture, bacteria[6], yeast[6,37], flies[6], worms[6], plants[35]	High temporal resolution due to high activity and tight control of user defined labeling window	Lower catalytic activity and stability compared with TurboID
Split-APEX2	Biotin phenol, hydrogen peroxide	≤1 min	Cytosol, nucleus, ER–mitochondria contact sites, cell surface[47]	Mammalian cell culture, yeast[47]	High reconstituted activity	Limited application in vivo due to reagent toxicity and low reagent permeability; requires supplementation of heme co-factor
Split-HRP	Biotin phenol, hydrogen peroxide	≤1 min	ER lumen, cell surface, neuronal synapse[48]	Mammalian cell culture, yeast[48]	High reconstituted activity	Limited application in vivo due to reagent toxicity and low reagent permeability; requires supplementation of heme co-factor; limited to secretory pathway and extracellular applications
Split-BioID	Biotin, ATP	18 h	Cytosol[49–51], nucleus[49], ER–mitochondria contact sites[51]	Mammalian cell culture	Non-toxic labeling conditions	Poor temporal resolution and very low catalytic activity
Split-TurboID	Biotin, ATP	1 h	Cytosol, nucleus, mitochondrial matrix, ER lumen, ER–mitochondria contact sites[7]	Mammalian cell culture	Non-toxic labeling conditions; higher reconstituted activity than split-BioID and full-length BioID	Lower catalytic activity compared with split peroxidase approaches

compartments such as the ER lumen[6,44,45]. Although newer ligases such as BioID2 and AirID have higher activity than BioID and BASU, they still require long labeling times and are much less active than TurboID or miniTurbo[6].

TurboID and miniTurbo have much faster labeling kinetics and higher labeling yields than any other biotin ligase-related PL method and have been shown to be active in several model organisms that were previously intractable to PL[6,35–37]. TurboID, which was evolved in the yeast secretory pathway, also has markedly higher activity in the ER lumen than BioID[6,45]. However, TurboID, which is the most active biotin ligase–based method, can exhibit biotinylation activity before addition of exogenous biotin because it can utilize endogenous biotin present in some cell types and organisms[6]. Although biotin is essential to several critical biological processes, such as fatty acid metabolism[46], endogenous concentrations of free biotin are typically too low for biotin ligase–based PL; however, different growth or culturing conditions can increase endogenous biotin concentrations. For example, cells cultured in biotin-rich medium such as RPMI 1640 or organisms that require dietary biotin supplementation will exhibit intracellular biotinylation by TurboID before the addition of exogenous biotin[6]. Conversely, organisms, such as bacteria, that regulate the biosynthesis of their own biotin will have lower concentrations of free biotin and therefore lower biotinylation by TurboID outside of the user-defined labeling window. Therefore, if a defined labeling time window is a priority for a given experiment (e.g., time course experiments, the study of particular points in development, or comparison of before versus after application of a stimulus), miniTurbo, which has lower biotin affinity and hence lower background labeling, can be used. Although miniTurbo is approximately twofold lower in activity as compared with TurboID, it still takes >100-fold shorter labeling times than BioID[6].

In some cases, the high activity and high biotin affinity of TurboID can cause cellular toxicity. For example, ubiquitous, constitutive expression of TurboID in all tissues throughout the fly can result in excessive sequestration of free biotin, which causes decreased survival and smaller fly size when grown without biotin supplementation[6]. This toxicity is ameliorated with biotin supplementation, with inducible TurboID expression, or when TurboID expression is restricted to specific tissues or organs. Furthermore, when TurboID labeling is carried out for >24 h in cultured mammalian cells (far longer than our recommended labeling time of 10 min), excessive biotinylation of the endogenous proteome can result in growth defects[6]. Therefore, a lower-activity PL method such as BioID or AirID may be beneficial in long-term experiments or in experiments in which biotin supplementation is problematic[26,31].

For applications in which the region of interest is inaccessible to traditional PL approaches, such as organelle contact sites, split PL methods, which can enable greater targeting specificity, can be used (Fig. 1b). Split PL approaches can also be applied when large protein fusions cannot be tolerated, because individual fragments can be much smaller. Split forms of APEX[47], HRP[48], BioID[49–51], and TurboID[7] have all been developed, in which two inactive fragments can reconstitute a full-length enzyme. With limitations similar to those of their full-length parental enzymes, split-APEX and split-HRP require H_2O_2 and heme addition, which limits their utility in vivo, and split-BioID has very low activity[7]. We recently developed split-TurboID, which has far higher activity than previous split-BioIDs[49–51] and is also more active than full-length BioID. We developed both low-affinity (PPI-dependent reconstitution) and high-affinity (PPI-independent reconstitution) versions of split-TurboID; split-TurboID-catalyzed PL with either version can be achieved with <1 h of biotin incubation[7]. Split variants of PL enzymes can be used for probing specific protein complexes[50] or mapping organelle contact sites[7,51], or can be further engineered to activate PL activity conditional to specific inputs, such as drug, light, or cell–cell contacts[7,48].

Biological applications of biotin ligase–related proximity labeling

Biotin ligase–related PL has been applied for proteomic mapping of a wide range of protein complexes and cellular structures, including the nuclear pore complex[30], transcriptional regulator complexes[52–54], the Hippo pathway[55], cilia[56], stress granules[57], centrosomes[58], pathological protein aggregates[59], viral and pathogen-associating protein interactomes[60–69], outer mitochondrial membrane (OMM)[70], ER–endosome contact sites[71], ER–plasma membrane contact sites[72], and ER–mitochondria contact sites[7,51]. These PL methods have also been used in a variety of cell types and species, including bacteria[6], yeast[37,39], plants[35], flies[6], worms[6], and mice[40,54,73,74]. These reported studies have enabled us to refine important technical considerations to guide future applications: (i) It is critical to experimentally validate that fusion to the PL enzyme does not disrupt the native function

and localization of the bait protein. (ii) For generation of the bait–enzyme fusion, CRISPR knock-in at the endogenous genomic locus or low-titer lentiviral delivery is preferred over transient transfection for minimizing artifacts arising from bait overexpression. (iii) The amount of input material (e.g., number of cells) and the labeling time need to be carefully gauged according to the size of the target proteome to ensure sufficient biotinylated material for MS detection with high depth of coverage.

Mass spectrometric data analysis

For proteomic mapping of numerous subcellular compartments in mammalian cells, we have found that the ratiometric approach[75] enables high spatial specificity for protein discovery. In this approach, the relative biotinylation of each protein by TurboID-fused bait is quantified relative to its biotinylation by a reference TurboID fusion construct. The reference construct should biotinylate a cellular or subcellular region that either is continuous with or overlaps with the target region of interest. For example, for mapping the proteome of the cytosol-facing endoplasmic reticulum (ER) membrane (ERM), cytosolic TurboID-NES was used as a reference[6]. As another example, for mapping the interactome of a transcription factor, TurboID fused to a nuclear localization sequence that targets it diffusely throughout the nucleus can be used as a reference. The quantitative comparison with the reference construct enables the identification of the subset of proteins that are preferentially biotinylated in the target region versus the reference region.

To process the mass spectrometric data and determine the final proteome lists, we use a receiver operating characteristic (ROC)-based analysis that applies curated lists of true-positive (TP) and false-positive (FP) proteins to establish optimal cutoffs. Cutoffs maximize the retention of TP proteins and minimize the retention of FP proteins in the final proteome lists.

We have previously used the ratiometric approach and ROC-based cutoff analysis with TurboID to generate highly specific proteome lists for the ERM[6]. The ratiometric approach has also been used in peroxidase-generated datasets for the mitochondrial intermembrane space[76], mitochondrial nucleoid[77], OMM[78], ER–mitochondria contact sites[7], and synaptic clefts[20] (Table 1, Supplementary Tables 1 and 2).

Although ROC-based cutoff analysis of PL data has proven powerful, increasing experimental complexity and the lack of extensive 'true positives' (gold standards) for many novel and underexplored subcellular compartments have prompted the need for more agnostic data analysis methods. For these types of experiments, various statistical approaches can be used to determine the variance of the signal while defining the background noise derived from various experimental artifacts, such as nonspecific labeling or imperfect subcellular localization. More straightforward experimental designs, such as examining the interactions of a PL enzyme-tagged bait protein compared with the background labeling of a free PL enzyme, can be analyzed using common statistical tests such as the one- or two-sample *t*-tests, which account for variability across small sample sets[10,79]. However, as the experimental design complexity increases, multivariate analyses using linear models can better account for added variables such as subcellular localization–specific protein–protein interactions. Multivariate analyses become the preferred statistical approach as additional control conditions are incorporated, eliminating the need for explicit pairing of experimental and control samples across a potentially mismatched number of replicates (e.g., three experimental replicates and two control replicates) and instead accounting for the variance across replicates for each experimental condition, as well as the variance across the various respective negative controls[80].

Because a wide range of statistical approaches can be adopted according to the experimental design, here we will focus specifically on data analysis using the ratiometric approach combined with ROC-based cutoff analysis, which can be applied to proteomic mapping of open cellular compartments[75].

Limitations and considerations

Different subcellular regions have distinct pH, redox environments, and endogenous nucleophile concentrations, which result in varying TurboID activity. For example, in HEK293T cells, TurboID has high activity in the cytosol and nucleus, whereas its activity in compartments such as the mitochondria and ER is lower[6]. Activity of TurboID also varies by the cell type chosen for cell culture and by organism[6]. For example, different growth conditions, media, and food required by different model organisms can change the experimental design necessary for maximal TurboID activity. Therefore, it is critical to assess the activity of the TurboID fusion construct to be used for proteomics

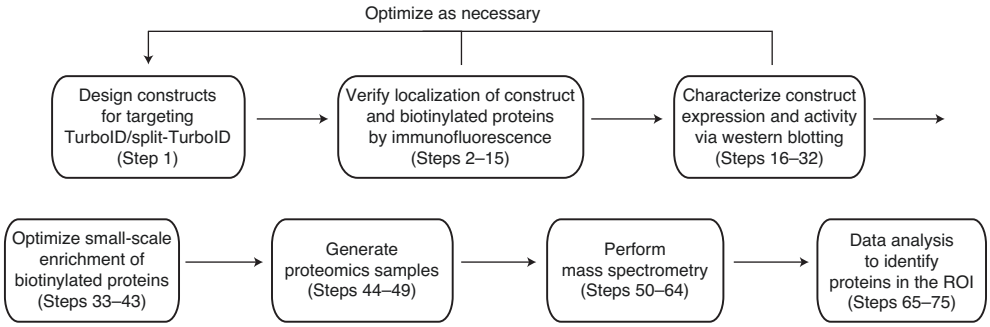

Fig. 2 | Workflow for performing a TurboID proteomic experiment. Designed fusion constructs should be characterized using immunofluorescence and western blot approaches and optimized as necessary. After construct validation, enrichment conditions need to be optimized before generating proteomic samples for mass spectrometric analysis. ROI, region of interest.

to ensure that it has sufficient activity in the biological context under investigation. Extending from this, TurboID can only label proteins with exposed, non-protonated amines, such as those on lysine side chains and N termini of proteins. Therefore, differences in pH and steric accessibility will affect the ability of a given protein to be labeled, which limits protein coverage.

Interactome mapping with PL methods, including TurboID, requires fusion of the protein of interest to the PL enzyme. This fusion may affect the stability, localization, function, and importantly, protein interactions of the protein of interest. Therefore, we advise that functional assays be performed to ensure that the TurboID fusion construct remains physiologically relevant and that its nature accurately reflects the endogenous protein being studied.

Finally, ratiometric and statistical analyses achieve high specificity by assessing the differential extent of biotinylation by a TurboID construct targeted to the region of interest versus TurboID targeted to a reference compartment. For example, a high-specificity proteome of the ERM was achieved by comparing the extent of biotinylation of proteins by TurboID targeted to the ERM versus TurboID expressed in the cytosol: true ERM proteins are more strongly biotinylated by ERM-TurboID versus cytosolic TurboID. Therefore, this analysis cannot account for proteins that are dual localized, which may result in lower coverage (e.g., a protein that resides on both the ERM and in the cytosol would be removed in the second filtering step using cytosolic TurboID as a reference).

Experimental Design

Overview of the procedure

The procedure described in this protocol consists of seven stages (Fig. 2 and Procedure). First, the fusion constructs are cloned (Step 1) and characterized by imaging (Steps 2–15) and western blot (Steps 16–32). Next, a small-scale enrichment of biotinylated proteins should be optimized (Steps 33–43) before generating and processing proteomic samples (Steps 44–49). Last, after mass spectrometric analysis (Steps 50–64), data analysis is performed to identify enriched proteins (Steps 65–75).

Targeting TurboID to the region of interest

To begin a proteomics experiment using TurboID or split-TurboID, the constructs first need to be targeted to the cellular region or protein complex of interest. For proteomic mapping of organelles or subcellular structures, targeting should be achieved by using localization sequences if possible. For example, we have targeted TurboID and split-TurboID to the ERM using targeting peptides derived from cytochrome P450 and cytochrome b5 (refs. [6,7]) and to the OMM using targeting peptides derived from mitochondrial antiviral-signaling protein (MAVS) and translocase of outer membrane 20-kDa subunit (Tom20) (refs. [6,7]; Fig. 3a,b). For organelle mapping, targeting to a subcellular region of interest via fusion to full-length, functional proteins should be avoided, if possible, because of the increased likelihood of perturbation of biological processes or signaling resulting from overexpression of a biologically active protein. Furthermore, although a given protein may be known to reside in the organelle or subcellular region of interest, its biological function or interactions may give the resulting TurboID or split-TurboID fusion constructs a unique localization pattern within that subcellular region that could bias the proteome being mapped. Multiple fusion constructs should be tested at different expression levels to ensure proper localization and minimal disruption of the targeted

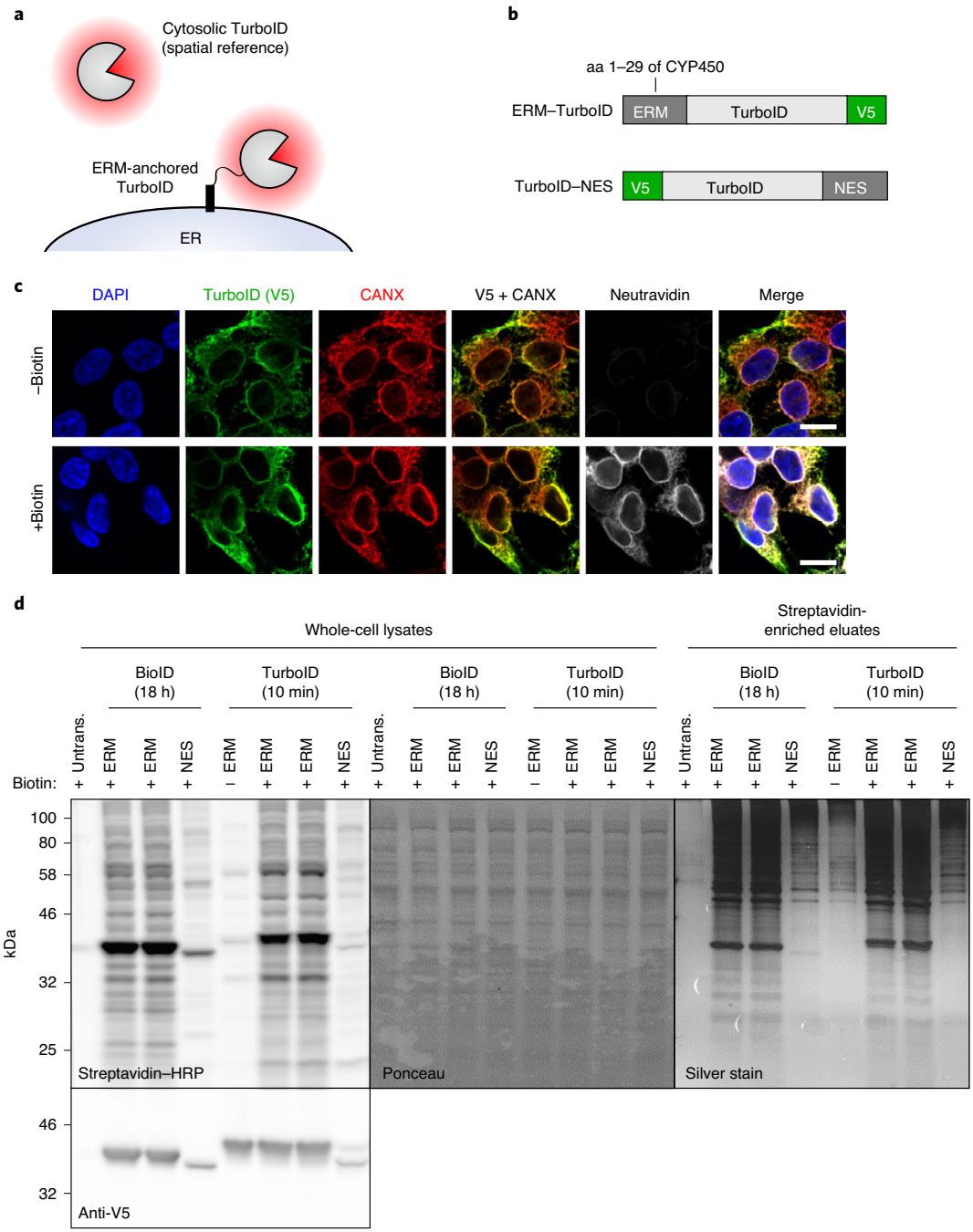

Fig. 3 | Example data characterizing ERM-targeted TurboID. a, TurboID targeted to the ERM for proteomic mapping. Cytosolic TurboID is used as a spatial reference control. **b**, ERM-targeted and cytosolic TurboID constructs. ERM–TurboID targeting sequence is derived from amino acids 1–29 of cytochrome P450 (CYP450). Cytosolic localization is achieved by fusion to a nuclear export sequence (NES). V5 epitope tags are included for construct detection in immunofluorescence and western blot experiments. **c**, Confocal fluorescence imaging of HEK293T cells stably expressing ERM-targeted TurboID. Cells were treated with 50 μM biotin for 10 min (+Biotin), and untreated cells (-Biotin) were used as a control. Cells were fixed and stained with an anti-V5 antibody to visualize ERM–TurboID localization, NeutrAvidin–Alexa Fluor 647 to visualize biotinylated proteins, and an anti-calnexin (CANX) antibody to visualize the ER (CANX is an endogenous ERM marker). ERM–TurboID colocalizes with endogenous CANX, and biotinylation activity is dependent on the addition of biotin. Scale bars, 10 μm. **d**, Characterization of biotinylation activity by ERM–TurboID. HEK293T cells stably expressing ERM–TurboID and TurboID–NES were treated with 50 μM biotin for 10 min and then lysed. Whole-cell lysates were analyzed by streptavidin–HRP blotting; Ponceau stain is included to show equal loading of total protein; streptavidin-enriched eluates were analyzed by silver stain. Biotinylation activity is dependent on the addition of exogenous biotin and ligase expression levels. Untransfected cells and cells expressing BioID constructs were included for comparison; TurboID with 10 min of biotin incubation achieves labeling comparable to that of BioID with 18 h of biotin incubation. **c**,**d**, Adapted with permission from ref. [6], Springer Nature America, Inc.

organelle. Localization of constructs can be verified by immunostaining and comparison with either a co-transfected/infected fluorescent protein marker targeting the same organelle or by co-immunostaining of endogenous markers in the targeted region (Fig. 3c). Alternatively, proper localization to particular organelles/components, such as the mitochondria, cytosol, nucleus, or ER, can be verified by comparison with one of our TurboID fusion constructs available via Addgene[6,7]. Additional optimization is required if the fusion construct does not colocalize with the targeted region or if substantial organelle perturbation is observed. Linker length, construct geometry, and targeting sequence can be altered if needed; expression levels can be optimized by using different approaches for introducing constructs. For example, we have seen that overexpression of constructs targeted to the ERM and OMM by Lipofectamine 2000 transfection can cause organelle aggregation, whereas lentiviral transduction or stable expression results in clean targeting to these locations with minimal organelle perturbation[6,7,76,78].

For expression of split-TurboID fragments, high overexpression can lead to proximity-independent reconstitution. Thus, lentivirus induction or stable construct expression should be used in most cases. Furthermore, although both fragments are tolerant of N- and C- terminal fusions, and there does not seem to be a preference in the pairing of different fusion constructs[7], optimization of different linkers and geometries may be necessary depending on the application.

To map the protein–protein interactions (PPIs) of a particular protein of interest (i.e., interactome mapping), TurboID or split-TurboID fragments are fused directly to the bait protein being studied. Here, it is critical to ensure that the fusion of TurboID/split-TurboID fragments does not perturb the localization pattern, biological functions, or interactions of the bait protein. For example, in PL studies using APEX2 to investigate GPCR signaling, APEX2-GPCR fusions were assayed to ensure that they retained proper trafficking, localization, and signaling capabilities[24,25]. Such control assays will be tailored to the bait protein being studied but may include immunofluorescence imaging to ensure proper trafficking and localization, functional assays to ensure there is no perturbation of signaling or biological function, and co-immunoprecipitation assays to ensure known PPIs are not disrupted. Proteins that have successfully been fused to GFP or similarly sized reporters will also probably tolerate fusion to TurboID (35 kDa) or to split-TurboID fragments (N-terminal fragment: 8 kDa; C-terminal fragment: 27 kDa).

For both applications of proteomic mapping outlined above, it is also critical to ensure that the TurboID or split-TurboID fusions do not affect ligase activity (see 'Characterizing activity of the TurboID construct'). This is not expected to be a common issue because both TurboID and split-TurboID are active as N-terminal or C-terminal fusions and retain activity in all cellular compartments tested[6,7]. However, if necessary, linkers can be used between fusion sites to aid in proper folding and maintain stability of the ligases; glycine and serine-rich linkers are typically used, with a length of 10 aa as a starting point. Altering linker length or rigidity (by changing amino acid composition) may be useful in optimizing the fusion constructs' expression or TurboID/split-TurboID activity. Epitope tags, such as V5 or HA, should be included in each fusion construct to enable detection via both immunofluorescence and western blot. Lysine-rich tags, such as the FLAG tag, should be avoided because they may be modified by TurboID labeling chemistry.

Characterizing activity of the TurboID construct

After verifying proper localization and/or function of the fusion construct, the activity of TurboID/split-TurboID needs to be evaluated. This can be done either by immunofluorescence staining of biotinylated proteins (e.g., using a fluorophore–NeutrAvidin conjugate) or by western blot analysis of biotinylated proteins from whole-cell lysate (e.g., using a streptavidin–fluorophore or streptavidin–HRP conjugate) (Fig. 3c,d). To perform labeling, cells expressing the desired constructs are incubated with 50–500 μM biotin. In HEK293T cells, TurboID labeling can be detected with 1–10 min of labeling, and split-TurboID labeling can be detected with 0.5–4 h of labeling[6,7]. Negative controls that omit the ligase or biotin should be included to assess signal from endogenously biotinylated proteins and background biotinylation levels. The labeling reaction is stopped by placing the cells on ice and washing out excess biotin.

It may be necessary to optimize labeling times and biotin concentrations according to the specific application. Furthermore, we advise that the lowest biotin concentration and shortest labeling time required for robust labeling be used, because higher concentrations and longer labeling times may result in saturation of nearby labeling sites, which may extend the labeling radius and reduce specificity[6,45]. Using the lowest concentration of exogenous biotin will also minimize the amount of free biotin that remains in the lysate at the time of enrichment (see below), as excess free biotin will

compete for binding sites on the streptavidin beads during enrichment, which can result in reduced capture of target biotinylated proteins.

For immunofluorescence imaging, cells should then be fixed and stained with a streptavidin– or NeutrAvidin–fluorophore conjugate to visualize biotinylated proteins. Staining against the fusion construct epitope tag should be included to visualize the localization of the fusion constructs. The streptavidin– or NeutrAvidin–fluorophore staining pattern should largely reflect where TurboID is expressed. For split-TurboID, the pattern of biotinylated proteins should reflect where both fragments are colocalized. The biotinylation signal may be detected beyond where TurboID/split-TurboID is localized; previous work from our group has shown that although specifically biotinylated proteins can migrate during the labeling reaction in live cells, the resulting proteomic data are still highly spatially specific[75,76].

Because the imaging assay described above cannot easily differentiate between ligase self-biotinylation and biotinylation of proximal endogenous proteins in the target region, labeling activity should also be checked by streptavidin blotting. For this assay, labeling is carried out in the same manner as described above (with the same negative controls). Whole-cell lysates generated from these samples are resolved by SDS-PAGE, and proteins are transferred onto a nitrocellulose membrane. Following blotting with a streptavidin–fluorophore or HRP conjugate and the necessary developing steps, a collection of bands representing biotinylated proteins should be observed spanning a large molecular weight range. For samples in which either ligase or biotin was omitted, only bands corresponding to endogenously biotinylated proteins should be visible (for human samples, at 72, 75, and 130 kDa[46]). Ideally, the intensity of bands representing endogenous proteins biotinylated by the TurboID fusion construct should be similar to or greater than the intensity of endogenous biotinylated protein bands; if so, this indicates efficient biotinylation by the TurboID fusion construct. However, if the fusion construct is expressed at very low levels, or if the fusion construct is localized to a compartment in which TurboID activity is low, it is possible that the bands will be faint; biotinylation is often sufficient, so long as the bands are visible and their signal is above those of the negative-control lanes. TurboID targeted to different subcellular regions may also show distinct banding patterns on the streptavidin blot, representative of the different labeled protein species. The same lysates should also be run and blotted with fluorophore/HRP–antibody conjugates against the appropriate epitope tag to verify expression and integrity (lack of proteolysis) of the TurboID fusion construct (Fig. 3d).

Next, a small-scale enrichment of proteins biotinylated by TurboID/split-TurboID should be performed because there are various experimental conditions that require optimization before a large-scale proteomic experiment. To perform the enrichment, whole-cell lysates generated from labeled cells are incubated with streptavidin-coated magnetic beads. After incubation, streptavidin beads are thoroughly washed under denaturing conditions, as detailed below. Biotinylated proteins are eluted from the beads by boiling in SDS protein-loading buffer supplemented with free biotin and dithiothreitol (DTT). The input and flow-through material are analyzed by streptavidin blotting to verify ligase- and biotin-dependent labeling and that biotinylated proteins were successfully extracted from the flow-through. The eluate samples are analyzed by silver stain to confirm successful enrichment of total protein in experimental samples as compared with negative controls (Fig. 3d). Optimization involving changing bead volume and the number of washes may be required to maximize capture of biotinylated material while minimizing nonspecific binding to the beads. Although the prescribed washing of cells after labeling in cell culture is often sufficient to remove free biotin that can inhibit the capture of biotinylated proteins, additional steps to remove free biotin—such as using gel filtration columns—can also be included before enrichment. Similarly, depletion of endogenously biotinylated proteins (e.g., carboxylases) before enrichment can be used to increase signal from TurboID/split-TurboID-labeled proteins[40].

The biotinylated material can also be probed for the enrichment of endogenous marker proteins by western blot. For example, we showed that BCAP31, a protein residing on the ERM, can be enriched from samples generated by ERM–TurboID[6] as compared with negative controls. In another example, we observed enrichment of ER–mitochondria contact resident proteins FACL4 and Mff from samples generated by split-TurboID constructs designed to map ER–mitochondria contact sites[7] as compared with negative controls. These data further support that biotinylation is spatially specific.

Sample preparation for proteomics

Optimized conditions from the small-scale enrichments can be scaled accordingly for the large-scale proteomics experiment. For proteomics experiments in HEK293T cells, we have used confluent T150

flasks (~20 million cells) to generate samples for mass spectrometric analysis[6,7]. Replicates should be included for each experimental condition. Negative controls that omit the ligase or biotin should also be included. To enable ratiometric or statistical analyses, it is also important to include controls for spatial specificity; for example, in our analysis of ERM proteins using TurboID or ER–mitochondria contact proteins using split-TurboID, we included samples with TurboID–NES localized to the cytosol for comparison[6] (Fig. 3a,d; Fig. 4; Fig. 5a–c).

As the affinity of streptavidin for biotin is exceptionally strong, we circumvent the need for elution of TurboID-biotinylated proteins from streptavidin beads for mass spectrometric analysis by releasing proteins coupled to the affinity matrix by a short on-bead digestion with trypsin or other proteolytic enzymes. After removal of streptavidin beads, released proteins are fully digested into peptides for analysis by liquid chromatography–tandem mass spectrometry (LC-MS/MS). Multiple quantitative or semi-quantitative approaches can be used to discriminate the enrichment of proteins in experimental conditions as compared with negative controls. Quantitative approaches, such as isobaric labeling of peptides, have been shown to be powerful technologies for PL-based enrichment experiments; here, we will focus on tandem mass tag (TMT)-based quantitation. Moreover, label-free approaches such as spectral counting, MS1 intensity/area under the curve, or targeted assays have also been used successfully[25,81,82].

Data analysis

For our standard data analysis pipelines, the raw mass spectrometry data are searched against a database of known proteins corresponding to the species used. Only proteins with two or more unique detected peptides are included for subsequent analysis.

For the ratiometric approach, two ROC-based filtering steps are required (i) to determine biotinylated proteins and (ii) to identify which proteins were preferentially labeled by TurboID targeted to a region of interest versus a reference control (Fig. 4b; Fig. 5d).

To determine the first cutoff, TMT ratios are calculated for each detected protein by dividing the TMT signal from the experimental sample by the TMT signal from the negative-control sample, in which proteins should not be biotinylated (omit-biotin control or omit-ligase control). The TMT ratios are then ranked from highest to lowest. Next, curated lists of TP and FP proteins, relevant to the interaction or subcellular compartment of interest, are generated on the basis of prior annotation and literature evidence. The TP list should include proteins expected to be biotinylated (e.g., proteins known to reside in the compartment being mapped or known to interact with the bait of interest), whereas the FP list should include proteins not expected to be biotinylated (e.g., proteins residing in a membrane-enclosed compartment that is inaccessible to the biotin–AMP intermediate generated by the TurboID-fusion construct in the experimental sample; e.g., we often use soluble mitochondrial matrix proteins as our FP list). Crossing these lists with the list of detected proteins enables determination of true and false positives present in the dataset. Next, at each possible TMT ratio cutoff, the TP rate (TPR) and the FP rate (FPR) are calculated, defined as the fraction of detected TP and FP proteins above the cutoff, respectively (Fig. 4b). Plotting the TPR versus the FPR in a ROC curve is informative for determining how well the proteomics experiment enriched TP over FP proteins. (Fig. 4c). The optimal cutoff ratio is then determined by maximizing TPR-FPR. Histograms plotting the distribution of TP and FP proteins in our dataset by TMT ratio should show that the ROC-determined cutoff successfully enriches TP proteins (Fig. 4c,d). Proteins above the determined TMT ratio cutoff are considered to be biotinylated proteins, whereas proteins below the cutoff are considered to be likely nonspecific binders.

We then perform a second filtering step, which has been shown to be important for maximizing the spatial specificity of our dataset[76]. The purpose of this filtering is to quantitatively compare the experimental sample with a reference control that targets TurboID to an overlapping, but distinct, subcellular region. For example, for mapping the ERM facing the cytosol, the data are first filtered using a control to account for the extent of biotinylation (omit-biotin or omit-ligase; described above) and then further filtered using a cytosolic TurboID reference control (Fig. 4e). For this second filtering, a second FP list (FP2) is required that contains proteins that could be biotinylated by the experimental sample TurboID–fusion construct (because they are in an adjacent or continuous compartment) but should be preferentially biotinylated by the reference control TurboID–fusion construct. For example, to map the ERM proteome, the reference control was cytosolic TurboID–NES, and the FP2 list contained non-secretory proteins, that is, proteins that are not predicted to be secretory by Phobius[83] or are not annotated with any Gene Ontology[84,85] terms

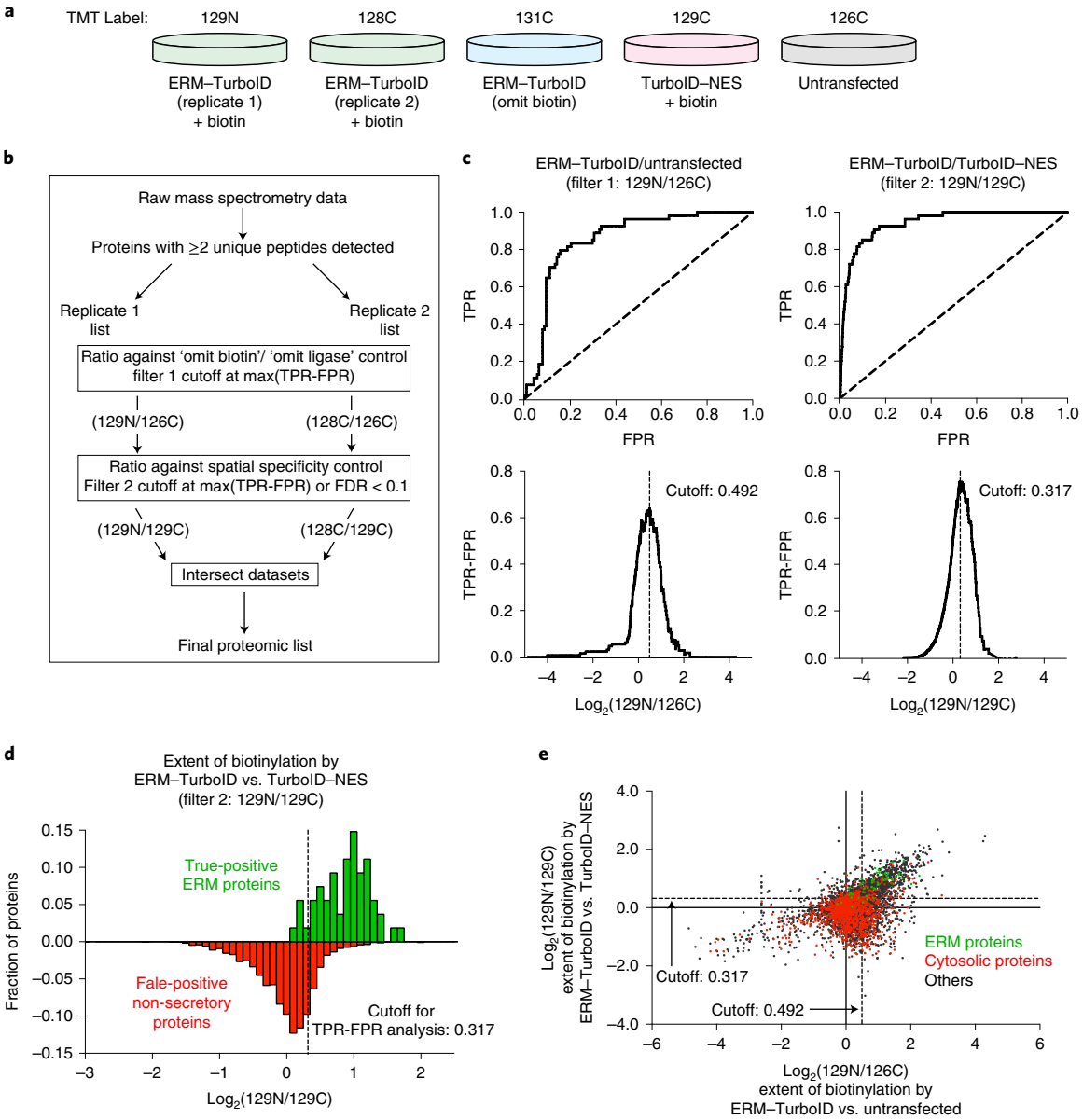

Fig. 4 | Proteomic data analysis using the ratiometric approach. a, Example experimental design for quantitative proteomic mapping of the ERM in HEK293T cells. The relevant subset of samples from ref. [6] is shown. **b**, Filtering scheme for mass spectrometric data. For each replicate, all proteins with ≥2 unique peptides are first filtered by whether or not they are biotinylated (ratiometric analysis referencing 'omit biotin' or 'omit ligase' controls, filter 1). Next, proteins were further filtered by the extent to which they are preferentially biotinylated in the target region versus the adjoining control region (ratiometric analysis referencing spatial reference controls, filter 2). Lists from each replicate, following application of two filters, are then intersected to generate the final proteome list. **c**, Establishing cutoffs for replicate 1 of the ERM–TurboID dataset. 129N corresponds to ERM–TurboID (replicate 1), and 129C corresponds to cytosolic TurboID–NES, both treated with 50 μM biotin for 10 min; 126C corresponds to the untransfected control. For each possible TMT ratio cutoff, the TPR was plotted versus the FPR in a ROC curve (top). True-positive proteins were previously annotated ERM proteins. For the first filter, previously annotated mitochondrial matrix proteins were used as FPs (FP1); for the second filter, previously annotated cytosolic (non-secretory) proteins were used as FPs (FP2). The optimal cutoffs were determined by the maximum TPR-FPR, indicated by dashed lines (bottom). **d**, Histograms of the distribution of true positive (TP) and false positive (FP) proteins. The distributions of TP ERM proteins and FP non-secretory proteins (from FP2) are plotted for the second ratiometric filtering step. The established cutoff, indicated by a dashed line, enriches TP over FP proteins. **e**, Scatter plot showing filter 1 (*x* axis) versus filter 2 (*y* axis) $\log_2$ ratios for each protein analyzed from ERM–TurboID. TMT ratio cutoffs used to obtain the filtered proteome, indicated by dashed lines, enrich previously annotated ERM proteins (green), relative to cytosolic (red) and other (black) proteins. Adapted with permission from ref. [6], Springer Nature America, Inc.

associated with secretory system organelles, for example, 'ER', 'Golgi', 'plasma membrane' (additional details can be found in the 'Methods' section of ref. [6]).

As before, TMT ratios are calculated for each detected protein by dividing the TMT signal from the experimental sample by the TMT signal from the reference control sample, and proteins are

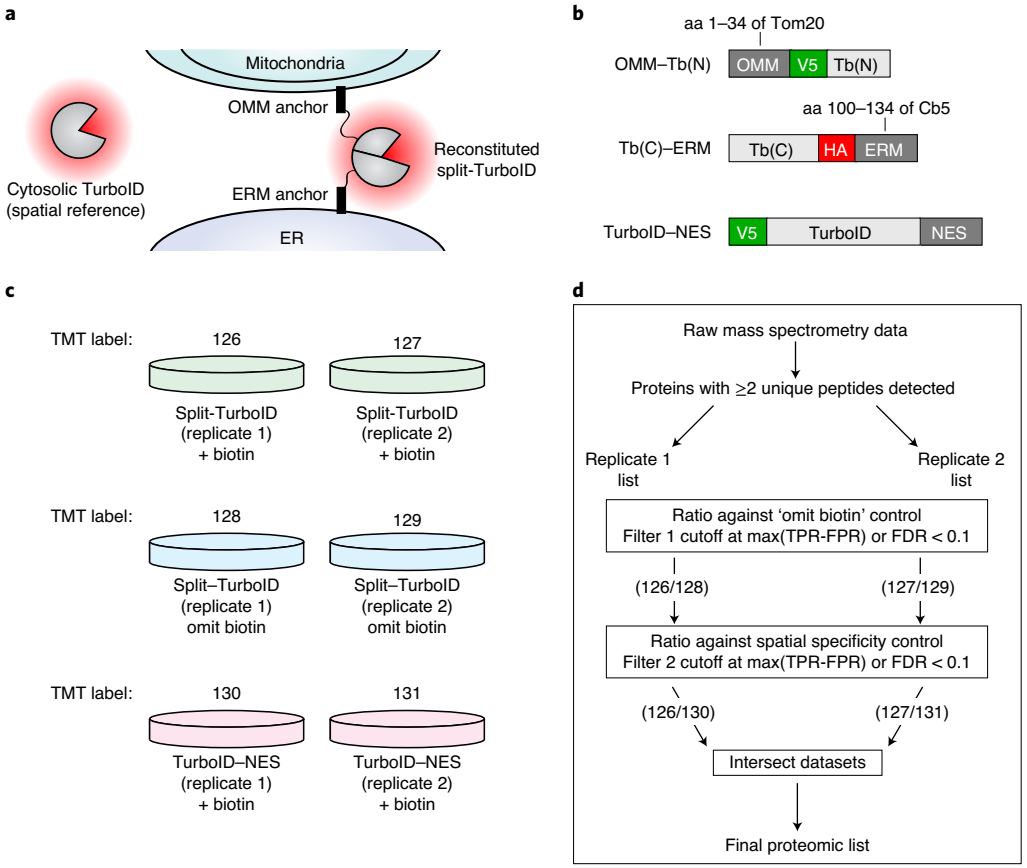

Fig. 5 | Example experimental design and analysis using split-TurboID for proteomic mapping of ER–mitochondria contacts. a, Split-TurboID targeted to ER–mitochondria contact sites for proteomic mapping in HEK293T cells[7]. Split-TurboID fragments are targeted to either the OMM or the ERM. Cytosolic TurboID is used as a spatial reference control. **b**, OMM- and ERM-targeted split-TurboID and cytosolic TurboID constructs. Tb(N) (N-terminal fragment) was targeted to the OMM using a targeting sequence derived from amino acids 1–34 of Tom20, and Tb(C) (C-terminal fragment) was targeted to the ERM using a targeting sequence derived from amino acids 100–134 of cytochrome b5 (Cb5), as described previously[7,47]. Cytosolic localization is achieved by fusion to a nuclear export sequence (NES). V5 and HA epitope tags are included for construct detection in immunofluorescence and western blot experiments. **c**, Example TMT 6-plex proteomic experimental design for mapping ER–mitochondria contacts. **d**, Filtering scheme for mass spectrometric data. For each replicate, all proteins with ≥2 unique peptides were first filtered by whether or not they are biotinylated (ratiometric analysis referencing 'omit biotin' controls, filter 1). Next, proteins were further filtered by their preferential labeling by split-TurboID at ER–mitochondria contacts versus cytosolic TurboID control (spatial specificity control; ratiometric analysis referencing TurboID–NES, filter 2). Lists from each replicate were then intersected to generate the final proteome list.

ranked from highest to lowest TMT ratio. ROC analysis and cutoff determination are performed as above. Both of these filtering steps should be repeated and applied to each independent replicate, and a final proteome list is generated from the intersection of the filtered lists from each replicate.

After obtaining a final proteome list, sensitivity and specificity analyses are performed to determine proteome quality. Sensitivity is typically calculated as the fraction of TP proteins detected in the final proteome. Specificity can be calculated as the fraction of the proteome that has prior annotation for the region of interest. Alternatively, specificity can be estimated using the false-discovery rate (FDR), which is based on the fraction of the proteome that contains verified false positives. Proteins that do not have prior annotation or literature support can be further validated by immunofluorescence imaging or western blot to determine their localization.

Materials

Biological materials

- Cell line of interest. In the example data shown in this protocol, we use human embryonic kidney (HEK) 293T cells (ATCC, cat. no. CRL-11268; RRID: CVCL_0063), as described in our published

studies[6,7]. We have also successfully used our approach with *E. coli* bacteria, *Saccharomyces cerevisiae* yeast, *Drosophila melanogaster* flies, and *Caenorhabditis elegans* worms, with appropriate protocol adaptations as described previously[6] **! CAUTION** Cell lines should be regularly checked to ensure they are mycoplasma negative.

Reagents

- TurboID plasmids, such as ERM- and cytosol-targeted constructs, can be obtained from Addgene (https://www.addgene.org/search/catalog/plasmids/?q=turboid)
- Split-TurboID plasmids, such as ERM- and OMM-targeted constructs, can be obtained from Addgene (https://www.addgene.org/search/catalog/plasmids/?q=split-turboid)
- DMEM (+4.5 g/L glucose, +L-glutamine, −sodium pyruvate; Corning, cat. no. 10-017-CV)
- Fetal bovine serum (FBS; VWR, cat. no. 97068-085)
- Penicillin–streptomycin (P/S; VWR, cat. no. 45000-652)
- GlutaMAX (Thermo Fisher Scientific, cat. no. 35050061)
- Lipofectamine 2000 (Thermo Fisher Scientific, cat. no. 11668019) or alternative transient transfection reagent
- Biotin (Sigma-Aldrich, cat. no. B4501)
- DMSO (Alfa Aesar, cat. no. AAJ66650AP)
- Fibronectin (human plasma purified; MilliporeSigma, cat. no. FC010)
- Dulbecco's phosphate-buffered saline (DPBS) (Thermo Fisher Scientific, cat. no. 21600010)
- Formaldehyde (10% (vol/vol); Ricca Chemical, cat. no. 3180-16) **! CAUTION** Formaldehyde is toxic and corrosive. Avoid contact with skin and eyes. Use in a chemical fume hood.
- PIPES sodium salt (MilliporeSigma, cat. no. 528131100GM)
- HEPES sodium salt (Thermo Fisher Scientific, cat. no. 15630080)
- EGTA (MilliporeSigma, cat. no. 32462625GM)
- Magnesium chloride ($MgCl_2$; VWR, cat. no. MK5958-04)
- Sucrose (VWR, cat. no. 0335-1kg)
- Methanol (MeOH; MilliporeSigma, cat. no. 34966-4L)
- Bovine serum albumin (BSA; Thermo Fisher Scientific, cat. no. BP16001)
- (Optional) Anti-V5 antibody (mouse; Thermo Fisher Scientific, cat. no. R96025; RRID: AB_2556564)
- (Optional) Anti-HA antibody (rabbit; Cell Signaling Technology, cat. no. C29F4; RRID: AB_1549585)
- NeutrAvidin biotin-binding protein (Thermo Fisher Scientific, cat. no. A2666)
- Alexa Fluor 647 NHS ester (Thermo Fisher Scientific, cat. no. A20006)
- (Optional) Anti-mouse Alexa Fluor 488 (goat; Thermo Fisher Scientific, cat. no. A11029; RRID: AB_2534088)
- (Optional) Anti-rabbit-Alexa Fluor 488 (goat; Thermo Fisher Scientific, cat. no. A11008; RRID: AB_143165)
- (Optional) Anti-mouse-Alexa Fluor 568 (goat; Thermo Fisher Scientific, cat. no. A11031; RRID: AB_144696)
- (Optional) Anti-rabbit-Alexa Fluor 568 (goat; Thermo Fisher Scientific, cat. no. A11036; RRID: AB_10563566)
- (Optional) Anti-mouse–horseradish peroxidase (HRP; goat; Bio-Rad, cat. no. 170-6516; RRID: AB_11125547)
- (Optional) Anti-rabbit–horseradish peroxidase (HRP; goat; Bio-Rad, cat. no. 170-6515; RRID: AB_11125142)
- Streptavidin–horseradish peroxidase (HRP; Thermo Fisher Scientific, cat. no. S911)
- (Optional) Anti-mouse IRDye 800 (goat; LI-COR, cat. no. 92632210; RRID: AB_621842)
- (Optional) Anti-rabbit IRDye 680 (goat; LI-COR, cat. no. 92568071; RRID: AB_2721181)
- (Optional) Streptavidin-IRDye 680 (LI-COR, cat. no. 92568079)
- Aqua-Mount mounting medium (Thermo Fisher Scientific, cat. no. 13800)
- Protease inhibitor cocktail (MilliporeSigma, cat. no. P8849-5ML)
- PMSF (phenylmethylsulfonyl fluoride; VWR, cat. no. 82021-256) **! CAUTION** PMSF is toxic. Avoid contact with skin or eyes.
- Isopropanol (VWR, cat. no. BDH1133-4LP)
- Nonfat dry milk (Thermo Fisher Scientific, cat. no. M0841)
- BCA Protein Assay Kit (Thermo Fisher Scientific, cat. no. 23225)
- ECL western blotting substrate (Bio-Rad, cat. no. 1705061)
- Tris hydrochloride (MilliporeSigma, cat. no. 10812846001)
- Glycerol (Thermo Fisher Scientific, cat. no. S25342D)
- Sodium dodecyl sulfate (SDS; MilliporeSigma, cat. no. L3771-1KG) **! CAUTION** Weigh SDS in a chemical fume hood.
- DTT (dithiothreitol; Thermo Fisher Scientific, cat. no. BP172-5)
- Bromophenol blue (MilliporeSigma, cat. no. B5525)

- TBST (20×; bioWORLD, cat. no. 40120065-2)
- Ponceau S (MilliporeSigma, cat. no. P-3504)
- Acetic acid (Thermo Fisher Scientific, cat. no. S25118) **! CAUTION** Acetic acid is corrosive. Avoid contact with skin or eyes.
- Silver stain kit (Thermo Fisher Scientific, cat. no. 24612) **! CAUTION** Silver stain is toxic. Avoid contact with skin or eyes.
- Streptavidin magnetic beads (Thermo Fisher Scientific, cat. no. 88817)
- Sodium bicarbonate (MilliporeSigma, cat. no. S6015-25G)
- Sodium chloride (NaCl; Thermo Fisher Scientific, cat. no. S271-10)
- Sodium deoxycholate (Thermo Fisher Scientific, cat. no. J6228822) **! CAUTION** Weigh sodium deoxycholate in a chemical fume hood.
- Triton X-100 (MilliporeSigma, cat. no. T9284-500ML)
- Potassium chloride (KCl; Thermo Fisher Scientific, cat. no. 7447-40-7)
- Sodium carbonate (Thermo Fisher Scientific, cat. no. S25539)
- Urea (VWR, cat. no. MK864806)
- Sequencing-grade modified trypsin (500 μg per vial or 5 × 20 μg per vial; Promega, cat. no. V511X or V5113)
- Formic acid (FA; Sigma-Aldrich, cat. no. 56302)
- Acetonitrile (J.T. Baker, cat. no. 9829-03)
- Iodoacetamide (Sigma-Aldrich, cat. no. A3221)
- TMT-10 Reagent Kit (Thermo Fisher Scientific, cat. no. 90110)
- HEPES (0.5 M buffer solution, pH 8.5; Alfa Aesar, cat. no. J63218)
- ReproSil-Pur 1.9-μm, C18 resin (Dr. Maisch GmbH)
- Hydroxylamine (50% (vol/vol); Sigma-Aldrich, cat. no. 467804) **! CAUTION** Hydroxylamine is an irritant. Avoid contact with skin or eyes and avoid inhalation.

Equipment

- Glass coverslips (Neuvitro, cat. no. GG-15-Pre)
- Centrifugal filter unit (Amicon Ultra-0.5; MilliporeSigma, cat. no. UFC503008)
- Plate for imaging cells (24 wells; VWR, cat. no. 10861-558)
- Plate for preparing western blot samples (6 wells; VWR, cat. no. 82050-842)
- Culture flasks for preparing proteomic samples (150 cm^2; VWR, cat. no. 430825)
- Tabletop centrifuge
- Floor centrifuge
- Fluorescence microscope with appropriate filter sets (we use a Zeiss AxioObserver inverted microscope with a 63× oil-immersion objective with the following combinations of laser excitation and emission filter sets: 405-nm laser excitation, 445/40-nm emission; 491-nm laser excitation, 528/38-nm emission; 561-nm laser excitation, 617/73-nm emission; 647-nm laser excitation, 680/30-nm emission)
- Magnetic rack for separation of magnetic beads (Thermo Fisher Scientific, cat. no. CS15000)
- Laboratory pipetting needles with 90° blunt ends (for use as a punch for separation materials to make StageTips), 16-gauge, 2-inch length (Cadence Science, cat. no. 7938)
- Tubing (PEEK, 25 μm × 1/32 inches × 5 feet, natural; Idex Health & Science, cat. no. 1567)
- StageTip C18 material (solid-phase C18 extraction disks, diameter = 47 mm; Empore, cat. no. 66883-U)
- Adaptor for StageTips (Glygen, cat. no. CEN.24)
- LC system for online LC-MS analysis **▲ CRITICAL** We use a Thermo Scientific Easy-nLC 1200 system and operate under ultra-performance liquid chromatography (UPLC) conditions. However, any LC system that can deliver nanoflow rates and can operate up to a pressure of 1,000 bar can be used for peptide separation.
- MS system for online LC-MS analysis (Thermo Fisher Scientific, Orbitrap Fusion Lumos model) **▲ CRITICAL** Although we use an Orbitrap Fusion Lumos, other LC-MS/MS systems can be used, as long as they have sufficient resolution in MS/MS mode to resolve the low-mass N and C series TMT-10 reporter ions. To resolve and accurately measure the near-isobaric N- and C-labeled reporter ions in the TMT-10 reagents, the instrument used must be able to achieve a minimum MS/MS resolution of 50,000 at $m/z = 150$.
- PicoFrit column (360-μm o.d. × 75 μm i.d., 10-μm i.d. tip, 50-cm length; New Objective, cat. no. PF360-75-10-N-5)

- Autosampler vial for LC-MS (300 µL; Waters, cat. no. 186002639)
- Autosampler cap for LC-MS (300 µL; Waters, cat. no. 186000305)
- Nanospray column heater (20 cm; Phoenix S&T, cat no. PST-CH-20U)
- Column heater controller (Phoenix S&T, cat. no. PST-CHC)
- Cell scraper
- Nitrocellulose or PVDF membranes

Software

- Spectrum Mill MS Proteomics Workbench v.6.0 (Agilent Technologies: https://www.agilent.com/en/products/software-informatics/mass-spectrometry-software/data-analysis/spectrum-mill)

▲ **CRITICAL** Although we used Spectrum Mill, other software packages that support the identification and quantification of high-resolution LC-MS/MS with TMT-10 reagents can be used.

Reagent setup

Complete DMEM medium

Supplement DMEM (+4.5 g/L glucose, +L-glutamine, −sodium pyruvate) medium with 10% (vol/vol) FBS, 1% (vol/vol) P/S, and 1% (vol/vol) GlutaMAX and filter-sterilize with a 0.2 µm filter. After filtering, complete DMEM medium can be stored at 4 °C for several months.

Biotin stock (100 mM)

Dissolve biotin in DMSO to a final concentration of 100 mM and make 200-µL aliquots. Aliquots can be stored at −20 °C for several months.

Tris-HCl (1 M)

Dissolve Tris hydrochloride in dH_2O and adjust the pH to 7.5 or 8.0, depending on its intended use. This solution can be stored at room temperature (RT: 20–22 °C) for several months.

PHEM buffer (5×)

Combine buffer ingredients (300 mM PIPES, 125 mM HEPES, 50 mM EGTA, 10 mM $MgCl_2$, 0.6 M sucrose) in dH_2O and adjust the pH to 7.3. This solution can be stored at 4 °C for many months.

Formaldehyde fixation solution (4% (vol/vol))

Dilute PHEM buffer (5×) 1:1 with non-supplemented DMEM and formaldehyde (10% (vol/vol)) to a final concentration of 1× PHEM buffer and 4% (vol/vol) formaldehyde. Alternatively, for strongly adherent cells such as HEK293T, (10% (vol/vol)) formaldehyde can also be diluted directly in DPBS to a final concentration of 4% (vol/vol). This solution should be freshly prepared before use.

NeutrAvidin–Alexa Fluor 647 conjugate

Mix 200 µL of 5 mg/mL NeutrAvidin in DPBS, 20 µL of 1 M sodium bicarbonate in water, and 10 µL of 10 mg/mL Alexa Fluor 647 NHS ester in DMSO and rotate in the dark for 3 h. Purify the NeutrAvidin–Alexa Fluor conjugate from unreacted dye by using an Amicon Ultra-0.5 filter unit according to the manufacturer's instructions. Collect the conjugate from the column using a total volume of 500 µL in DPBS. The eluted conjugate can be stored in the dark at 4 °C for several months.

RIPA lysis buffer

Combine buffer ingredients (50 mM Tris, 150 mM NaCl, 0.1% (wt/vol) SDS, 0.5% (wt/vol) sodium deoxycholate, 1% (vol/vol) Triton X-100) in dH_2O and adjust the pH to 7.5 This solution can be stored at 4 °C for many months.

PMSF (100 mM)

Dissolve PMSF in isopropanol to a final concentration of 100 mM and make 100-µL aliquots. Aliquots can be stored at −20 °C for several months.

Protein loading buffer (6×)

Combine buffer ingredients (0.33 M Tris (pH 6.8), 34% (vol/vol) glycerol, 10% (wt/vol) SDS, 0.09% (wt/vol) DTT, 0.12% (wt/vol) bromophenol blue) in dH_2O and make 1-mL aliquots. Aliquots can be stored at −20 °C for several months

Ponceau S stain
Combine ingredients (1 mg/mL Ponceau S, 5% (vol/vol) acetic acid) in dH_2O. This solution can be stored at room temperature for several months and can be reused several times.

TBST (1×)
Dissolve 20× TBST in dH_2O (final concentration of TBST is 0.1% (vol/vol)). This solution can be stored at room temperature for several months.

KCl (1 M)
Dissolve KCl in dH_2O to a final concentration of 1 M. This can be stored at room temperature for several months.

Na_2CO_3 (0.1 M)
Dissolve sodium carbonate (Na_2CO_3) in dH_2O to a final concentration of 0.1 M. This solution should be made fresh before use.

Urea (2 M) in 10 mM Tris-HCl (pH 8.0)
Dissolve urea in 10 mM Tris-HCl (pH 8.0) to a final concentration of 2 M. This solution should be made fresh before use.

DTT stock (1 M)
Dissolve DTT in dH_2O to a final concentration of 1 M. This solution can be stored at −20 °C for several months.

StageTip solvents
StageTip solvents are 0.1% (vol/vol) FA and 50% (vol/vol) acetonitrile (solvent 1) and 0.1% (vol/vol) FA (solvent 2). These solutions can be stored at room temperature for several weeks.

LC-MS/MS solvents
Solvent A is 0.1% (vol/vol) FA and 3% (vol/vol) acetonitrile. Solvent B is 0.1% (vol/vol) FA and 90% (vol/vol) acetonitrile. These solutions can be stored at room temperature for 2 weeks.

Equipment setup

Liquid chromatography settings
Solvents A and B are described in the 'Reagent setup' section. The settings in Table 2 are specific to a nanospray column packed up to 24 cm with ReproSil-Pur 1.9 μm, C18 resin. If another LC system is used, it may be necessary to adjust these parameters.

Mass spectrometer settings
The settings in Table 3 are specific to an Orbitrap Fusion Lumos. If another MS system is used, it may be necessary to adjust these parameters.

Parameters for searching MS data
Table 4 contains the parameters for searching MS data.

Procedure

Generation of TurboID/split-TurboID fusion constructs ● Timing variable

1 Design fusion constructs with desired linkers, epitope affinity tags, and localization sequences as discussed in the 'Experimental design' section. Avoid FLAG and other lysine-rich epitope tags that may be disrupted by TurboID labeling chemistry. TurboID/split-TurboID fusion constructs can be introduced into mammalian cells by transfection or viral transduction; transfection/infection efficiency should be maximized, because untransfected cells may contribute to background signal. Generating cell lines stably expressing fusion constructs by selection may be necessary to achieving optimal expression levels for maximizing labeling activity without perturbing organelle morphology.
? TROUBLESHOOTING

Table 2 | Liquid chromatography settings

Time interval (min)	Gradient (%B)	Flow rate (nL/min)
0	2	200
1	6	200
235	30	200
244	60	200
245	90	200
250	90	200
251	50	500
260	50	500

Table 3 | Mass spectrometer settings

Method/parameter	Value
Full MS	
Microscans	1
Resolution	60,000
Automatic gain control (AGC) target	3×10^6 ion counts
Scan range	350–1,800 *m/z*
Data-dependent mode	Cycle time
dd-MS2	
Microscans	1
AGC target	1×10^5 ion counts
Maximum ion time	120 ms
Isolation window	0.7 *m/z*
Fixed first mass	100 *m/z*
HCD energy (%)	36
dd settings	
Monoisotopic peak determination	Peptide
Charge exclusion	Include 2–6 charge states
Exclude isotopes	On
Dynamic exclusion	45 s

dd, data dependent.

Characterization of fusion constructs by imaging ● Timing 3–5 d

2 Place glass coverslips into 24-well plates and coat with 300 µL of 50 µg/mL human fibronectin solution in DPBS for at least 30 min at room temperature to improve cell adherence.

3 Remove the fibronectin solution and wash the coverslips with 500 µL DPBS. Plate cells onto glass coverslips with 500 µL complete DMEM medium. In the case of HEK293T cells, we plate either ~60,000 cells/well for transfection the next day or ~120,000 cells/well (using stable cells) for biotin labeling the next day.

▲ **CRITICAL STEP** Prepare additional coverslips to include negative controls that omit either the ligase (in Step 4) or the biotin (in Step 5). For testing split-TurboID constructs, additional negative controls, in which the expressed fusion constructs should not interact, and positive controls using full-length TurboID can be included.

4 (Optional) This step can be skipped if stable cell lines are being used. When cells are adhered to the coverslips, introduce fusion constructs either by transfection using Lipofectamine 2000 according to the manufacturer's instructions or by lentiviral infection as previously described[6,7]. Include co-transfection/co-infection of fluorescent protein markers if necessary (i.e., mCherry-KDEL as an ER marker); alternatively, immunostain endogenous markers at Step 10. Ideally, cells should be at ~70% confluency at the time of transfection or ~50% confluency at the time of viral infection.

Table 4 | Parameters for searching MS data

Parameter	Value
Variable modification	Oxidation (M)
	Acetyl (protein N-terminus)
Fixed modification	Carbamidomethyl (C)
	TMT-10 (peptide N-term, K)
Digest	Trypsin
Maximum missed cleavages	4
Maximum charge	6
Precursor mass tolerance (p.p.m.)	20
Product mass tolerance (p.p.m.)	20
Peptide FDR (%)	1

5 Either 24 h after transfection with Lipofectamine 2000 or 48 h after viral infection, replace the medium in each well with warm biotin-containing complete DMEM medium to initiate labeling (made fresh; final concentration = 50 μM biotin; adjust if necessary up to 500 μM biotin). Incubate cells with biotin at 37 °C for the desired time. TurboID labeling can be detected within 1–10 min of labeling, and split-TurboID labeling can be detected within 0.5–4 h of labeling[6,7]. Although these labeling times are good starting points, it may be necessary to optimize labeling according to the application.

6 Stop the labeling reaction by moving the cells onto ice and washing five times with 500 μL ice-cold (4 °C) DPBS.

7 Fix the cells with 500 μL formaldehyde fixation solution for 15 min on ice.

8 Permeabilize the cells with 500 μL ice-cold methanol at −20 °C for 5 min.

9 Wash the cells three times with 500 μL ice-cold DPBS and block with 500 μL 1% (wt/vol) BSA in DPBS at 4 °C for at least 30 min.

10 Remove the solution and incubate with primary antibody in 300 μL 1% (wt/vol) BSA in DPBS at 4 °C for 1 h. For V5 or HA detection, use a 1:1,000 dilution of mouse anti-V5 antibody or rabbit anti-HA antibody. Include antibodies for endogenous markers if necessary.

11 Gently wash the cells three times with 500 μL 1% (wt/vol) BSA in DPBS.

12 Incubate with fluorophore-conjugated secondary antibody in 300 μL 1% (wt/vol) BSA in DPBS at 4 °C for 1 h. Stain for biotinylated proteins using a NeutrAvidin–fluorophore conjugate in the same solution (1:1,000 dilution).

13 Gently wash the cells three times with 500 μL 1% (wt/vol) BSA in DPBS.

14 Mount coverslips onto a glass slide using mounting medium and allow to set overnight at room temperature in the dark.

PAUSE POINT Mounted coverslips can be stored in the dark at 4 °C for at least a month.

15 Image the coverslips using a fluorescence microscope with appropriate filter settings. Compare ligase immunostaining patterns and NeutrAvidin staining patterns with organelle markers to determine localization of constructs.

? TROUBLESHOOTING

Characterization of fusion constructs by western blot ● Timing 3–5 d

16 Plate fresh cells into 6-well plates; in the case of HEK293T cells, we plate either ~300,000 cells/well for transfection the next day or ~600,000 cells/well (using stable cells) for biotin labeling the next day.

▲ CRITICAL STEP Prepare additional wells to include negative controls that omit either the ligase (in Step 4) or the biotin (in Step 5). For testing split-TurboID constructs, additional negative controls in which the expressed fusion constructs should not interact and positive controls using full-length TurboID can be included.

17 Introduce fusion constructs and perform biotin labeling as described in Steps 4–6.

18 Gently wash the samples five times on ice with 1 mL ice-cold DPBS.

19 Use 1 mL ice-cold DPBS per well to detach cells via pipetting and collect the cell suspension into microcentrifuge tubes. A cell scraper may need to be used for strongly adherent cells.
20 Pellet the cells by centrifugation at 300*g* at 4 °C for 3 min and remove the supernatant.
21 Lyse the cell pellets with 100 µL RIPA lysis buffer supplemented with 1× protease inhibitor cocktail and 1 mM PMSF. Ensure the pellets are resuspended well by pipetting, and then incubate on ice for ≥10 min.
22 Clarify cell lysates by centrifugation at 13,000*g* at 4 °C for 10 min and transfer the clarified lysates to fresh microcentrifuge tubes. Protein concentration can be assessed by BCA protein assay to ensure even loading onto the SDS gel in Step 24.
23 Combine whole-cell lysates with 6× protein loading buffer and boil the samples at 95 °C for 10 min.
24 Load ~10–30 µg protein per sample and separate the proteins on a 9% (vol/vol) SDS polyacrylamide gel. Run two separate gels; one will be used to detect protein biotinylation, and the other gel will be used to detect expression of the fusion construct.
25 Transfer the proteins to a nitrocellulose membrane (PVDF membranes can also be used but may have lower adsorption of high-molecular-weight proteins).
26 Stain with Ponceau S solution to verify the quality of the transfer and that protein loading is comparable between samples. Destain with deionized water and rinse once with 1× TBST.
27 Block with 5% (wt/vol) nonfat dry milk in 1× TBST while rocking at room temperature for 1 h.
28 Wash the membranes three times with 1× TBST for 5 min each.
29 For detecting protein biotinylation, incubate with 0.3 µg/mL streptavidin–HRP in 3% (wt/vol) BSA in 1× TBST at room temperature for 30 min (nonfat dry milk should not be used for this incubation because it contains free biotin, which may interfere with streptavidin binding to adsorbed biotinylated proteins). Alternatively, incubate with streptavidin–IRDye conjugates (1:3,000) for imaging using LI-COR imaging systems.
30 For detecting expression of the fusion constructs, incubate with mouse anti-V5 (1:10,000) or rabbit anti-HA (1:5,000) antibody in 3% (wt/vol) BSA in 1× TBST at room temperature for 1 h or at 4 °C overnight. Wash the membrane three times with 1× TBST for 5 min each. Incubate with secondary antibody in 3% (wt/vol) BSA in 1× TBST at room temperature for 30 min.
31 Wash the membranes three times with 1× TBST for 5 min each.
32 Develop the membranes using ECL western blotting substrate for 1 min; then image. If LI-COR conjugates are being used, wash the membrane with DPBS (without Tween 20) two additional times for 5 min each. Image the membrane using the LI-COR imaging system.
? TROUBLESHOOTING

Optimization of protein enrichment before proteomics ● Timing 4–6 d

33 Generate labeled whole-cell lysates as described in Steps 16–22.
34 Estimate the amount of protein in each sample in triplicate using the BCA protein assay.
35 For each sample, take 25 µL streptavidin magnetic beads and wash twice with 1 mL RIPA lysis buffer.
36 Incubate the beads with 300 µg protein from each sample with an additional 500 µL RIPA lysis buffer at 4 °C for at least 1 h with rotation. The enrichment step can also be performed overnight. Save the remaining material (store at −20 °C) from the whole-cell lysates for western blot analysis in Step 42 (input).
37 After enrichment, pellet the beads, using a magnetic rack, and collect the supernatant in fresh microcentrifuge tubes for western blot analysis in Step 42 (flow-through).
38 Wash the beads twice with RIPA lysis buffer (1 mL, 2 min at RT), once with 1 M KCl (1 mL, 2 min at RT), once with 0.1 M Na_2CO_3 (1 mL, ~10 s), once with 2 M urea in 10 mM Tris-HCl (pH 8.0) (1 mL, ~10 s), and twice with RIPA lysis buffer (1 mL per wash, 2 min at RT). Do not allow the beads to sit for extended times in Na_2CO_3 or urea because extended periods tend to denature the beads and cause aggregation. After the final wash, transfer the beads in 1 mL RIPA lysis buffer to fresh tubes.
39 Elute the enriched material from the beads by boiling each sample in 30 µL of 3× protein loading buffer supplemented with 2 mM biotin and 20 mM DTT at 95 °C for 10 min.
40 Pellet the beads, using a magnetic rack, and collect the eluate.
41 Combine the input (from Step 36) and the flow-through (from Step 37) samples with 6× protein loading buffer and boil the samples at 95 °C for 10 min.

42 Run input, flow-through, and eluate samples on a 9% (vol/vol) SDS polyacrylamide gel and perform streptavidin–HRP blotting as described in Steps 24–32. Check that biotinylated proteins have been depleted from the flow-through and enriched in the eluate. A second gel can be used to run eluate samples and to determine whether endogenous protein markers have been successfully enriched.
? TROUBLESHOOTING

43 Run eluate samples on a 9% (vol/vol) SDS polyacrylamide gel and perform a silver staining to visualize the amount of total proteins in each lane. More proteins should have been enriched from the experimental samples than from negative-control samples. The amount of streptavidin beads and labeling time can be further optimized on the basis of the results in this step.
? TROUBLESHOOTING

Preparation of proteomic samples ● Timing 5–7 d

44 Design the proteomic experiment with the appropriate controls and number of replicates. Negative controls should be included in which either the ligase or the biotin is omitted. Replicates should be included at least for the experimental sample(s) of interest.

45 Expand mammalian cell cultures; for proteomic experiments in HEK293T cells, one T150 flask is typically used per condition (~20 million cells).

46 (Optional) If stable cells are not being used, transfect or transduce the cells with fusion constructs using previously optimized conditions (while scaling up appropriately).

47 Label the cells with biotin using the previously optimized conditions and then move the samples onto ice.

48 Perform enrichment as previously described in Steps 33–38 (while scaling up the amount of streptavidin beads (e.g., 250 µL per T150 flask, but amounts can be adjusted according to optimization in Steps 33–43).
▲ CRITICAL STEP Retain 2.5% of the whole-cell lysate before enrichment to verify ligase expression and confirm biotinylation by western blot according to Steps 22–32.

49 Take 5% of the washed streptavidin beads to verify protein enrichment by silver stain as described in Steps 39–41 and 43. Proceed to on-bead trypsin digestion with the rest of the sample.
? TROUBLESHOOTING

Mass spectrometry ● Timing 2 d

50 To prepare proteomic samples for mass spectrometry analysis, wash the proteins bound to streptavidin beads with 200 µL of 50 mM Tris-HCl (pH 7.5), followed by two washes with 200 µL 2M urea in 50 mM Tris (pH 7.5) buffer. The wash buffer volumes may need to be increased dependent on the final volume of streptavidin beads.

51 Remove the final volume of 2 M urea in 50 mM Tris (pH 7.5) buffer and incubate the beads with 80 µL of 2 M urea in 50 mM Tris-HCL containing 1 mM DTT and 0.4 µg trypsin at 25 °C for 1 h while shaking at 1,000 r.p.m.

52 After 1 h, remove the supernatant and transfer to fresh tubes.

53 Wash streptavidin beads twice with 60 µL of 2 M urea in 50 mM Tris (pH 7.5) buffer and combine the washes with the on-bead digest supernatant from Step 52.

54 Reduce the disulfide bonds in the eluent by adding DTT to a final concentration of 4 mM and incubate at 25 °C for 30 min with shaking at 1,000 r.p.m.

55 Alkylate the eluent by adding iodoacetamide to a final concentration of 10 mM and incubate at 25 °C for 45 min in the dark while shaking at 1,000 r.p.m.

56 Add an additional 0.5 µg of trypsin to the sample and let digestion proceed overnight at 25 °C with shaking at 700 r.p.m.

57 After overnight digestion, acidify the sample by adding FA such that the sample contains ~1% (vol/vol) FA and is at pH 3.

58 Desalt the samples using C18 StageTips as previously described[86]. Briefly, condition C18 StageTips with 100 µL of 100% MeOH, 100 µL of solvent 1, and twice with 100 µL of solvent 2. Load acidified peptides onto the conditioned StageTips and wash twice with 100 µL of solvent 2. Elute the peptides from the StageTips with 50 µL of solvent 1 and vacuum centrifuge the samples at room temperature until completely dry.

59 Label the desalted peptides with TMT reagents as follows: Reconstitute peptides in 100 µL of 50 mM HEPES. Reconstitute each 0.8-mg vial of TMT reagent in 41 µL of anhydrous acetonitrile

and add the reagent to the corresponding peptide sample. Let the reactions proceed at room temperature for 1 h.

60 Quench the TMT-labeling reactions with 8 µL of 5% (vol/vol) hydroxylamine at room temperature for 15 min with shaking.

61 Evaporate TMT-labeled samples to dryness in a vacuum concentrator and desalt the peptides on C18 StageTips exactly as described in Step 58.

62 Reconstitute each TMT-labeled sample in 9 µL of 0.1% (vol/vol) FA/3% (vol/vol) acetonitrile and place it in the LC autosampler.

63 Set up a nanospray column packed up to 24 cm with ReproSil-Pur 1.9 µm, C18 resin. Use the column heater to heat the column to 50 °C.

64 Set up the Orbitrap Fusion Lumos using the parameters provided in the 'Equipment setup' section. Run the LC system with the solvents and gradient described in the 'Reagent setup' and 'Equipment setup' sections. For each analysis, we typically inject half of each sample, saving half in case a reinjection is needed.

Data analysis ● Timing 1 week

65 Analyze the MS data from the TMT experiments. We typically use the Spectrum Mill MS Proteomics Workbench. Typical parameters used for searching data with Spectrum Mill are provided in the 'Equipment setup' section.

? TROUBLESHOOTING

66 For the ratiometric approach, analyze each replicate separately and overlap the lists at the end to obtain a final proteome list. Begin with all proteins that were identified by two or more unique peptides.

67 Generate lists of TP and FP proteins. For a three-state ratiometric analysis approach, two lists of FP proteins are required for two filtering steps: one for proteins that should not be biotinylated by TurboID and another for proteins that do not localize to the cellular compartment being analyzed. Comprehensive lists of TP and FP proteins can be generated by combining information from the Gene Ontology Cellular Component (GOCC) database[84], the UniProt database[87], and the literature. For example, for the analysis of proteomic data generated from ERM–TurboID, the first filter step compared ERM–TurboID with untransfected controls and used a FP list containing mitochondrial matrix proteins, whereas the second step compared ERM–TurboID with cytosolic TurboID–NES and used a FP list containing non-secretory system proteins[6] (Fig. 4c–e).

68 Normalize corresponding TMT ratios against the distribution of FP proteins that should not be biotinylated by TurboID. To do this, divide all TMT ratios by the median of the ratios for FP proteins. Calculate the $\log_2$ value of each ratio; $\log_2$ values will be used for the rest of the analysis. This normalization centers the distribution of the $\log_2$ ratios of nonspecifically binding proteins around 0.

69 Check the correlation between replicates by plotting the corresponding $\log_2$ ratios.

70 Rank the proteins by the appropriate TMT ratio values in descending order and cross this list with the TP and FP lists to determine which proteins are TPs and FPs, respectively.

71 At each potential cutoff, calculate the TPR and FP rate (FPR), where the TPR/FPR is defined as the number of detected TP/FP proteins detected above the cutoff divided by the total number of detected TP/FP proteins in that replicate. A plot of the TPR versus the FPR should show that the curve bows out as compared with the diagonal, which shows that the proteomic experiment successfully enriched TP proteins over FP proteins (Fig. 4c).

72 Determine the cutoff by using the $\log_2$ ratio that corresponds to the maximum TPR-FPR value. In cases in which the list of TP proteins is small (e.g., ER–mitochondria contacts; Fig. 5a–d), the cutoff can be alternatively determined with a FDR cutoff (Fig. 5d), where FDR is defined as the fraction of FP proteins detected above each cutoff.

73 Retain all proteins with $\log_2$ ratios higher than that of the determined cutoff.

74 For a three-state ratiometric experiment, take the list of proteins from Step 73 and repeat Steps 70–73 with a different set of TMT ratios and FP list (appropriate for the desired analysis).

? TROUBLESHOOTING

75 After filtering, overlap the protein lists from each replicate to obtain the final proteome.

Troubleshooting

Troubleshooting advice can be found in Table 5.

Table 5 | Troubleshooting table

Step	Problem	Possible reason	Solutions
1	Fusion construct is not properly targeted to the organelle/region of interest	Targeting sequence does not work	Try either an alternative targeting sequence or an alternative fusion location
			Try to avoid targeting sequences that are lysine rich
		Expression level of the fusion construct is too high	Reduce the expression level (switching promoters, changing transfection approaches, generating stable cells)
	Expression of the fusion construct disrupts the organelle/region of interest	Expression level of the fusion construct is too high	Reduce the expression level (switching promoters, changing transfection approaches, generating stable cells)
		Fusion construct design is disruptive	For targeting and localization to an organelle/region of interest, instead of using full-length proteins, try to fuse minimal peptide sequences that retain targeting, but not biological activity
15	Fusion construct is inactive	Either the construct is not expressed or the expression level of the construct is too low	Immunostain for the epitope tag to verify expression
			Expression can be optimized by using alternative targeting sequences/fusion sites, including or altering linkers between proteins fused, or changing promoters or methods of transfection
		Biotin labeling protocol or streptavidin/NeutrAvidin staining protocol is incorrect	Confirm that labeling works by using a positive control (TurboID or split-TurboID constructs can be obtained from Addgene)
	Fusion construct is not detectable by immunostaining	Expression level is too low	Expression can be optimized by using alternative targeting sequences/fusion sites, including or altering linkers between proteins fused, or changing promoters or methods of transfection
32	Fusion construct is inactive	Either the construct is not expressed or the expression level of the construct is too low	Immunoblot for the epitope tag to verify expression
			Expression can be optimized by using alternative targeting sequences/fusion sites, including or altering linkers between proteins fused, or changing promoters or methods of transfection
		Biotin labeling protocol or streptavidin staining protocol is incorrect	Confirm that labeling works by using a positive control (TurboID or split-TurboID constructs can be obtained from Addgene)
42	Poor enrichment of biotinylated proteins	Excess biotin in the cell lysate is competing for binding to streptavidin beads	Increase the number of washes and their duration
			Experimentally determine the minimal concentration of exogenous biotin required for robust labeling
		Amount of sample used for enrichment is not sufficient	Increase the amount of input material
		Not enough streptavidin beads were used	Increase the amount of streptavidin beads for capturing biotinylated proteins
		Elution is ineffective	Check that the concentration of free biotin in the sample buffer is correct
			Increase the boiling time as necessary
43, 49	High background signal in negative controls	Excessive non-specific protein binding to streptavidin beads	Increase the number, volume, and/or duration of washing steps
			Try more stringent washing conditions, such as higher urea concentrations
			Reduce the amount of streptavidin beads used; determine the minimal amount of beads that can be used while still capturing all biotinylated proteins (flow-through is cleared) and use that amount
65	Low yield of biotinylated proteins	Amount of sample used for enrichment is not sufficient	Increase the amount of input material
		Not enough streptavidin beads were used	Increase the amount of streptavidin beads for capturing biotinylated proteins
		Elution by on-bead digestion was ineffective	Check the pH of the digestion buffer
			Increase the amount of trypsin used for on-bead digestion

Table continued

Table 5 (continued)

Step	Problem	Possible reason	Solutions
74	Resulting ROC curve is not smooth	The TP or FP lists are too small	Try to build TP and FP lists as large as possible For mapping regions with low numbers of true positives, the cutoff can be alternatively determined with an FDR cutoff
	The histogram of log_2 ratios comparing the experimental condition to the 'omit-biotin' or 'omit-ligase' controls do not show a right-shift for true positives	Biotinylation was unsuccessful	Additional testing or optimization may be required (see Troubleshooting advice for Steps 32, 42, 43, 49)
		Excessive nonspecific protein binding to streptavidin beads or inefficient protein enrichment	Additional testing or optimization may be required (see Troubleshooting advice for Steps 42, 43, 49)
	The histogram of log_2 ratios comparing the experimental condition with spatial specificity controls do not show a right-shift for true positives	Poor spatial specificity in this experiment	Ensure that the fusion construct localizes properly to the region of interest Test that the fusion construct can preferentially biotinylate known proteins in the region of interest as compared with controls (Step 42)
		Expected proteome size may be small, resulting in less marked separation	Strongly enriched proteins may still be genuine hits; additional experimental validation is required

Timing

Generation of TurboID/split-TurboID fusion constructs
Step 1: variable
Characterization of fusion constructs by imaging
Steps 2–4: 1–3 d (timing depends on use of stable cells, transfection, or infection)
Steps 5–13: 1 d
Steps 14 & 15: 1 d
Characterization of fusion constructs by western blot
Steps 16 & 17: 1–3 d
Steps 18–23: 2 h
Steps 24–26: 4 h
Steps 27–32: 3 h + 1 h or overnight for Step 30
Optimization of protein enrichment before proteomics
Step 33: 2–4 d
Steps 34–41: 1 d
Steps 42 & 43: 1 d
Preparation of proteomic samples
Steps 44–47: 3–5 d
Step 48: 1 d
Step 49: 1 d
Mass spectrometric data acquisition
Steps 50–64: 2 d
Data analysis
Steps 65–75: 1 week

Anticipated results

Properly targeted TurboID or split-TurboID fusion constructs should colocalize with appropriate markers. Example confocal fluorescence imaging of ERM-targeted TurboID and biotin-dependent labeling is shown in Fig. 3c. TurboID biotinylation should be dependent on biotin addition; split-TurboID biotinylation should be dependent on both biotin addition and protein–protein or organelle–organelle interactions to drive reconstitution. Example streptavidin–HRP blot and silver stain of streptavidin-enriched material are shown in Fig. 3d.

For a successful proteomics experiment, TP proteins should have higher TMT ratios than FP proteins, and so a ROC plot should show the TPR increasing faster than the FPR (Fig. 4c). Plotting

the distributions of TP and FP proteins should also show that the established TMT ratio cutoffs successfully enrich TP proteins (Fig. 4d,e). For example, in the proteomic mapping of the ERM, using cutoffs defined by the maximum TPR-FPR, there is a clear enrichment of ERM proteins over cytosolic proteins. For mapping regions with fewer known true positives, such as ER–mitochondria contact sites (Fig. 5a–d), the cutoff can be alternatively determined with an FDR cutoff. Candidate proteins generated from proteomics experiments should be validated using independent approaches—such as by imaging, pull-downs, or functional assays—to confirm they are genuine hits.

Reporting Summary

Further information on research design is available in the Nature Research Reporting Summary linked to this article.

Data availability

The data presented in this paper have been previously published, and associated raw data are provided in the original articles[6,7].

References

1. Huber, L. A., Pfaller, K. & Vietor, I. Organelle proteomics: implications for subcellular fractionation in proteomics. *Circ. Res.* **92**, 962–968 (2003).
2. Puig, O. et al. The tandem affinity purification (TAP) method: a general procedure of protein complex purification. *Methods* **24**, 218–229 (2001).
3. Stasyk, T. & Huber, L. A. Zooming in: fractionation strategies in proteomics. *Proteomics* **4**, 3704–3716 (2004).
4. Lee, W. C. & Lee, K. H. Applications of affinity chromatography in proteomics. *Anal. Biochem.* **324**, 1–10 (2004).
5. Gingras, A. C., Abe, K. T. & Raught, B. Getting to know the neighborhood: using proximity-dependent biotinylation to characterize protein complexes and map organelles. *Curr. Opin. Chem. Biol.* **48**, 44–54 (2019).
6. Branon, T. C. et al. Efficient proximity labeling in living cells and organisms with TurboID. *Nat. Biotechnol.* **36**, 880–887 (2018).
7. Cho, K. F. et al. Split-TurboID enables contact-dependent proximity labeling in cells. *Proc. Natl Acad. Sci. USA* **117**, 12143–12154 (2020).
8. Udeshi, N. D. et al. Antibodies to biotin enable large-scale detection of biotinylation sites on proteins. *Nat. Methods* **14**, 1167–1170 (2017).
9. Fazal, F. M. et al. Atlas of subcellular RNA localization revealed by APEX-Seq. *Cell* **178**, 473–490.e26 (2019).
10. Myers, S. A. et al. Discovery of proteins associated with a predefined genomic locus via dCas9-APEX-mediated proximity labeling. *Nat. Methods* **15**, 437–439 (2018).
11. Michalski, A. et al. Mass spectrometry-based proteomics using Q Exactive, a high-performance benchtop quadrupole Orbitrap mass spectrometer. *Mol. Cell. Proteom.* **10**, M111.011015 (2011).
12. Eliuk, S. & Makarov, A. Evolution of Orbitrap mass spectrometry instrumentation. *Annu. Rev. Anal. Chem.* **8**, 61–80 (2015).
13. Tyanova, S., Temu, T. & Cox, J. The MaxQuant computational platform for mass spectrometry-based shotgun proteomics. *Nat. Protoc.* **11**, 2301–2319 (2016).
14. Lam, S. S. et al. Directed evolution of APEX2 for electron microscopy and proximity labeling. *Nat. Methods* **12**, 51–54 (2014).
15. Rhee, H. W. et al. Proteomic mapping of mitochondria in living cells via spatially restricted enzymatic tagging. *Science* **339**, 1328–1331 (2013).
16. Mortensen, A. & Skibsted, L. H. Importance of carotenoid structure in radical-scavenging reactions. *J. Agric. Food Chem.* **45**, 2970–2977 (1997).
17. Wishart, J. F. & Rao, B. S. M. *Recent Trends in Radiation Chemistry* (World Scientific, 2010). https://doi.org/10.1142/7413
18. Martell, J. D. et al. Engineered ascorbate peroxidase as a genetically encoded reporter for electron microscopy. *Nat. Biotechnol.* **30**, 1143–1148 (2012).
19. Rodríguez-López, J. N. et al. Mechanism of reaction of hydrogen peroxide with horseradish peroxidase: identification of intermediates in the catalytic cycle. *J. Am. Chem. Soc.* **123**, 11838–11847 (2001).
20. Loh, K. H. et al. Proteomic analysis of unbounded cellular compartments: synaptic clefts. *Cell* **166**, 1295–1307.e21 (2016).
21. Bar, D. Z. et al. Biotinylation by antibody recognition—a method for proximity labeling. *Nat. Methods* **15**, 127–133 (2018).
22. Honke, K. & Kotani, N. The enzyme-mediated activation of radical source reaction: a new approach to identify partners of a given molecule in membrane microdomains. *J. Neurochem* **116**, 690–695 (2011).

23. Li, X.-W. et al. New insights into the DT40 B cell receptor cluster using a proteomic proximity labeling assay. *J. Biol. Chem.* **289**, 14434–14447 (2014).
24. Paek, J. et al. Multidimensional tracking of GPCR signaling via peroxidase-catalyzed proximity labeling. *Cell* **169**, 338–349.e11 (2017).
25. Lobingier, B. T. et al. An approach to spatiotemporally resolve protein interaction networks in living cells. *Cell* **169**, 350–360.e12 (2017).
26. Roux, K. J., Kim, D. I., Raida, M. & Burke, B. A promiscuous biotin ligase fusion protein identifies proximal and interacting proteins in mammalian cells. *J. Cell Biol.* **196**, 801–810 (2012).
27. Kim, D. I. et al. An improved smaller biotin ligase for BioID proximity labeling. *Mol. Biol. Cell* **27**, 1188–1196 (2016).
28. Ramanathan, M. et al. RNA-protein interaction detection in living cells. *Nat. Methods* **15**, 207–212 (2018).
29. Choi-Rhee, E., Schulman, H. & Cronan, J. E. Promiscuous protein biotinylation by *Escherichia coli* biotin protein ligase. *Protein Sci.* **13**, 3043–3050 (2008).
30. Kim, D. I. et al. Probing nuclear pore complex architecture with proximity-dependent biotinylation. *Proc. Natl Acad. Sci. USA* **111**, E2453–E2461 (2014).
31. Kido, K. et al. Airid, a novel proximity biotinylation enzyme, for analysis of protein–protein interactions. *eLife* **9**, e54983 (2020).
32. Birendra, K. C. et al. VRK2A is an A-type lamin-dependent nuclear envelope kinase that phosphorylates BAF. *Mol. Biol. Cell* **28**, 2241–2250 (2017).
33. Redwine, W. B. et al. The human cytoplasmic dynein interactome reveals novel activators of motility. *eLife* **6**, e28257 (2017).
34. Jung, E. M. et al. Arid1b haploinsufficiency disrupts cortical interneuron development and mouse behavior. *Nat. Neurosci.* **20**, 1694–1707 (2017).
35. Mair, A., Xu, S. L., Branon, T. C., Ting, A. Y. & Bergmann, D. C. Proximity labeling of protein complexes and cell type specific organellar proteomes in *Arabidopsis* enabled by TurboID. *eLife* **8**, e47864 (2019).
36. Zhang, Y. et al. TurboID-based proximity labeling reveals that UBR7 is a regulator of N NLR immune receptor-mediated immunity. *Nat. Commun.* **10**, 3252 (2019).
37. Larochelle, M., Bergeron, D., Arcand, B. & Bachand, F. Proximity-dependent biotinylation mediated by TurboID to identify protein-protein interaction networks in yeast. *J. Cell Sci.* **132**, jcs232249 (2019).
38. Struk, S. et al. Exploring the protein–protein interaction landscape in plants. *Plant Cell Environ.* **42**, 387–409 (2019).
39. Opitz, N. et al. Capturing the Asc1p/receptor for activated C kinase 1 (RACK1) microenvironment at the head region of the 40s ribosome with quantitative BioID in yeast. *Mol. Cell. Proteom.* **16**, 2199–2218 (2017).
40. Uezu, A. et al. Identification of an elaborate complex mediating postsynaptic inhibition. *Science* **353**, 1123–1129 (2016).
41. Lin, Q. et al. Screening of proximal and interacting proteins in rice protoplasts by proximity-dependent biotinylation. *Front. Plant Sci.* **8**, 749 (2017).
42. Khan, M., Youn, J. Y., Gingras, A. C., Subramaniam, R. & Desveaux, D. In planta proximity dependent biotin identification (BioID). *Sci. Rep.* **8**, 1123 (2018).
43. Conlan, B., Stoll, T., Gorman, J. J., Saur, I. & Rathjen, J. P. Development of a rapid in planta bioid system as a probe for plasma membrane-associated immunity proteins. *Front. Plant Sci.* **9**, 1882 (2018).
44. Roux, K. J., Kim, D. I., Burke, B. & May, D. G. BioID: a screen for protein-protein interactions. *Curr. Protoc. Protein Sci.* **91**, 19.23.1–19.23.15 (2018).
45. May, D. G., Scott, K. L., Campos, A. R. & Roux, K. J. Comparative application of BioID and TurboID for protein-proximity biotinylation. *Cells* **9**, 1070 (2020).
46. Chapman-Smith, A. & Cronan, J. E. Jr Molecular biology of biotin attachment to proteins. *J. Nutr.* **129**, 477S–484S (1999).
47. Han, Y. et al. Directed evolution of split APEX2 peroxidase. *ACS Chem. Biol.* **14**, 619–635 (2019).
48. Martell, J. D. et al. A split horseradish peroxidase for the detection of intercellular protein-protein interactions and sensitive visualization of synapses. *Nat. Biotechnol.* **34**, 774–780 (2016).
49. De Munter, S. et al. Split-BioID: a proximity biotinylation assay for dimerization-dependent protein interactions. *FEBS Lett.* **591**, 415–424 (2017).
50. Schopp, I. M. et al. Split-BioID a conditional proteomics approach to monitor the composition of spatiotemporally defined protein complexes. *Nat. Commun.* **8**, 15690 (2017).
51. Kwak, C. et al. Contact-ID, a new tool for profiling organelle contact site, reveals proteins of mitochondrial-associated membrane formation. *Proc. Natl Acad. Sci. USA* **117**, 12109–12120 (2020).
52. McClellan, D. et al. Growth factor independence 1B-mediated transcriptional repression and lineage allocation require lysine-specific demethylase 1-dependent recruitment of the BHC complex. *Mol. Cell. Biol.* **39**, e00020-19 (2019).
53. Lambert, J. P. et al. Interactome rewiring following pharmacological targeting of BET bromodomains. *Mol. Cell* **73**, 621–638.e17 (2019).
54. Dingar, D. et al. BioID identifies novel c-MYC interacting partners in cultured cells and xenograft tumors. *J. Proteom.* **118**, 95–111 (2015).

55. Couzens, A. L. et al. Protein interaction network of the mammalian hippo pathway reveals mechanisms of kinase-phosphatase interactions. *Sci. Signal.* **6**, rs15–rs15 (2013).
56. Gupta, G. D. et al. A dynamic protein interaction landscape of the human centrosome-cilium interface. *Cell* **163**, 1484–1499 (2015).
57. Youn, J. Y. et al. High-density proximity mapping reveals the subcellular organization of mRNA-associated granules and bodies. *Mol. Cell* **69**, 517–532.e11 (2018).
58. Firat-Karalar, E. N., Rauniyar, N., Yates, J. R. & Stearns, T. Proximity interactions among centrosome components identify regulators of centriole duplication. *Curr. Biol.* **24**, 664–670 (2014).
59. Chou, C. C. et al. TDP-43 pathology disrupts nuclear pore complexes and nucleocytoplasmic transport in ALS/FTD. *Nat. Neurosci.* **21**, 228–239 (2018).
60. Kabeiseman, E. J., Cichos, K. H. & Moore, E. R. The eukaryotic signal sequence, YGRL, targets the chlamydial inclusion. *Front. Cell. Infect. Microbiol.* **4**, 129 (2014).
61. Mojica, S. A. et al. SINC, a type III secreted protein of *Chlamydia psittaci*, targets the inner nuclear membrane of infected cells and uninfected neighbors. *Mol. Biol. Cell* **26**, 1918–1934 (2015).
62. Le Sage, V., Cinti, A., Valiente-Echeverría, F. & Mouland, A. J. Proteomic analysis of HIV-1 Gag interacting partners using proximity-dependent biotinylation. *Virol. J.* **12**, 138 (2015).
63. Ritchie, C., Cylinder, I., Platt, E. J. & Barklis, E. Analysis of HIV-1 Gag protein interactions via biotin ligase tagging. *J. Virol.* **89**, 3988–4001 (2015).
64. Kueck, T. et al. Serine phosphorylation of HIV-1 Vpu and its binding to tetherin regulates interaction with clathrin adaptors. *PLoS Pathog.* **11**, e1005141 (2015).
65. Holthusen, K., Talaty, P. & Everly, D. N. Regulation of latent membrane protein 1 signaling through interaction with cytoskeletal proteins. *J. Virol.* **89**, 7277–7290 (2015).
66. Coyaud, E. et al. Global interactomics uncovers extensive organellar targeting by Zika virus. *Mol. Cell. Proteom.* **17**, 2242–2255 (2018).
67. Rider, M. A. et al. The interactome of EBV LMP1 evaluated by proximity-based BioID approach. *Virology* **516**, 55–70 (2018).
68. Cheerathodi, M. R. & Meckes, D. G. BioID combined with mass spectrometry to study herpesvirus protein–protein interaction networks. *Methods Mol. Biol.* **2060**, 327–341 (2020).
69. Bradley, P. J., Rayatpisheh, S., Wohlschlegel, J. A. & Nadipuram, S. M. Using BioID for the identification of interacting and proximal proteins in subcellular compartments in *Toxoplasma gondii*. *Methods Mol. Biol.* **2071**, 323–346 (2020).
70. Gillingham, A. K., Bertram, J., Begum, F. & Munro, S. In vivo identification of GTPase interactors by mitochondrial relocalization and proximity biotinylation. *eLife* **8**, e45916 (2019).
71. Hoyer, M. J. et al. A novel class of ER membrane proteins regulates ER-associated endosome fission. *Cell* **175**, 254–265.e14 (2018).
72. van Vliet, A. R. et al. The ER stress sensor PERK coordinates ER-plasma membrane contact site formation through interaction with filamin-A and F-actin remodeling. *Mol. Cell* **65**, 885–899.e6 (2017).
73. Spence, E. F. et al. In vivo proximity proteomics of nascent synapses reveals a novel regulator of cytoskeleton-mediated synaptic maturation. *Nat. Commun.* **10**, 386 (2019).
74. Feng, W. et al. Identifying the cardiac dyad proteome in vivo by a BioID2 knock-in strategy. *Circulation* **141**, 940–942 (2020).
75. Hung, V. et al. Spatially resolved proteomic mapping in living cells with the engineered peroxidase APEX2. *Nat. Protoc.* **11**, 456–475 (2016).
76. Hung, V. et al. Proteomic mapping of the human mitochondrial intermembrane space in live cells via ratiometric APEX tagging. *Mol. Cell* **55**, 332–341 (2014).
77. Han, S. et al. Proximity biotinylation as a method for mapping proteins associated with mtDNA in living cells. *Cell Chem. Biol.* **24**, 404–414 (2017).
78. Hung, V. et al. Proteomic mapping of cytosol-facing outer mitochondrial and ER membranes in living human cells by proximity biotinylation. *eLife* **6**, e24463 (2017).
79. Mertins, P. et al. Reproducible workflow for multiplexed deep-scale proteome and phosphoproteome analysis of tumor tissues by liquid chromatography-mass spectrometry. *Nat. Protoc.* **13**, 1632–1661 (2018).
80. Li, J. et al. Cell-surface proteomic profiling in the fly brain uncovers wiring regulators. *Cell* **180**, 373–386.e15 (2020).
81. Vandemoortele, G. et al. A well-controlled BioID design for endogenous bait proteins. *J. Proteome Res.* **18**, 95–106 (2019).
82. Bian, Y. et al. Robust, reproducible and quantitative analysis of thousands of proteomes by micro-flow LC–MS/MS. *Nat. Commun.* **11**, 157 (2020).
83. Käll, L., Krogh, A. & Sonnhammer, E. L. L. A combined transmembrane topology and signal peptide prediction method. *J. Mol. Biol.* **338**, 1027–1036 (2004).
84. Ashburner, M. et al. Gene ontology: tool for the unification of biology. *Nat. Genet.* **25**, 25–29 (2000).
85. Gene Ontology Consortium. Gene Ontology Consortium: going forward. *Nucleic Acids Res.* **43**, D1049–D1056 (2015).
86. Rappsilber, J., Mann, M. & Ishihama, Y. Protocol for micro-purification, enrichment, pre-fractionation and storage of peptides for proteomics using StageTips. *Nat. Protoc.* **2**, 1896–1906 (2007).
87. Bateman, A. et al. UniProt: the universal protein knowledgebase. *Nucleic Acids Res* **45**, D158–D169 (2017).

88. Lee, S. Y. et al. APEX fingerprinting reveals the subcellular localization of proteins of interest. *Cell Rep.* **15**, 1837–1847 (2016).
89. Cho, I. T. et al. Ascorbate peroxidase proximity labeling coupled with biochemical fractionation identifies promoters of endoplasmic reticulum–mitochondrial contacts. *J. Biol. Chem.* **292**, 16382–16392 (2017).
90. Cao, Q. et al. PAQR3 regulates endoplasmic reticulum-to-Golgi trafficking of COPII vesicle via interaction with Sec13/Sec31 coat proteins. *iScience* **9**, 382–398 (2018).
91. Le Guerroué, F. et al. Autophagosomal content profiling reveals an LC3C-dependent piecemeal mitophagy pathway. *Mol. Cell* **68**, 786–796.e6 (2017).
92. Mick, D. U. et al. Proteomics of primary cilia by proximity labeling. *Dev. Cell* **35**, 497–512 (2015).
93. Santin, Y. G. et al. In vivo TssA proximity labelling during type VI secretion biogenesis reveals TagA as a protein that stops and holds the sheath. *Nat. Microbiol.* **3**, 1304–1313 (2018).
94. Mannix, K. M., Starble, R. M., Kaufman, R. S. & Cooley, L. Proximity labeling reveals novel interactomes in live *Drosophila* tissue. *Development* **146**, dev176644 (2019).
95. Liu, G. et al. Mechanism of adrenergic CaV1.2 stimulation revealed by proximity proteomics. *Nature* **577**, 695–700 (2020).
96. Chojnowski, A. et al. Progerin reduces LAP2α-telomere association in Hutchinson-Gilford progeria. *eLife* **4**, 1–21 (2015).
97. Cross, S. H. et al. The nanophthalmos protein TMEM98 inhibits MYRF self-cleavage and is required for eye size specification. *PLoS Genet* **16**, e1008583 (2020).
98. Pagac, M. et al. SEIPIN regulates lipid droplet expansion and adipocyte development by modulating the activity of glycerol-3-phosphate acyltransferase. *Cell Rep.* **17**, 1546–1559 (2016).
99. Cole, A. et al. Inhibition of the mitochondrial protease ClpP as a therapeutic strategy for human acute myeloid leukemia. *Cancer Cell* **27**, 864–876 (2015).
100. Janer, A. et al. SLC 25A46 is required for mitochondrial lipid homeostasis and cristae maintenance and is responsible for Leigh syndrome. *EMBO Mol. Med.* **8**, 1019–1038 (2016).
101. Antonicka, H. et al. A pseudouridine synthase module is essential for mitochondrial protein synthesis and cell viability. *EMBO Rep.* **18**, 28–38 (2017).
102. Van Itallie, C. M. et al. Biotin ligase tagging identifies proteins proximal to E-cadherin, including lipoma preferred partner, a regulator of epithelial cell-cell and cell-substrate adhesion. *J. Cell Sci.* **127**, 885–895 (2014).
103. Guo, Z. et al. E-cadherin interactome complexity and robustness resolved by quantitative proteomics. *Sci. Signal.* **7**, rs7 (2014).
104. Hua, R. et al. VAPs and ACBD5 tether peroxisomes to the ER for peroxisome maintenance and lipid homeostasis. *J. Cell Biol.* **216**, 367–377 (2017).
105. Chan, C. J. et al. BioID performed on Golgi enriched fractions identify C10orf76 as a GBF1 binding protein essential for Golgi maintenance and secretion. *Mol. Cell. Proteom.* **18**, 2285–2297 (2019).
106. Opitz, N. et al. Capturing the Asc1p/ *R* eceptor for *A* ctivated *C K* inase *1* (RACK1) microenvironment at the head region of the 40S ribosome with quantitative BioID in yeast. *Mol. Cell. Proteom.* **16**, 2199–2218 (2017).
107. Domsch, K. et al. The hox transcription factor ubx stabilizes lineage commitment by suppressing cellular plasticity in *Drosophila*. *eLife* **8**, e42675 (2019).
108. Bagchi, P., Torres, M., Qi, L. & Tsai, B. Selective EMC subunits act as molecular tethers of intracellular organelles exploited during viral entry. *Nat. Commun.* **11**, 1127 (2020).
109. Yoshinaka, T. et al. Structural basis of mitochondrial scaffolds by prohibitin complexes: insight into a role of the coiled-coil region. *iScience* **19**, 1065–1078 (2019).
110. Callegari, S. et al. A MICOS–TIM22 association promotes carrier import into human mitochondria. *J. Mol. Biol.* **431**, 2835–2851 (2019).
111. Chen, Z. et al. Global phosphoproteomic analysis reveals ARMC10 as an AMPK substrate that regulates mitochondrial dynamics. *Nat. Commun.* **10**, 104 (2019).
112. Liu, L., Doray, B. & Kornfeld, S. Recycling of Golgi glycosyltransferases requires direct binding to coatomer. *Proc. Natl Acad. Sci. USA.* **115**, 8984–8989 (2018).
113. Mirza, A. N. et al. LAP2 proteins chaperone GLI1 movement between the lamina and chromatin to regulate transcription. *Cell* **176**, 198–212.e15 (2019).

Acknowledgements

This work was supported by NIH R01-DK121409 (to A.Y.T. and S.A.C.) and the Stanford Wu Tsai Neurosciences Institute Big Ideas Initiative (to A.Y.T.). K.F.C. was supported by NIH Training Grant 2T32CA009302-41 and the Blavatnik Graduate Fellowship. T.C.B. is a Robert Black Fellow of the Damon Runyon Cancer Research Foundation (DRG-2391-20). A.Y.T. is an investigator of the Chan Zuckerberg Biohub.

Author contributions

K.F.C., T.C.B, N.D.U., S.A.M., S.A.C., and A.Y.T. contributed to the writing and editing of the manuscript.

Competing interests

A.Y.T. and T.C.B. have filed a patent application covering some aspects of this work.

Additional information

Supplementary information is available for this paper at https://doi.org/10.1038/s41596-020-0399-0.

Correspondence and requests for materials should be addressed to A.Y.T.

Received: 17 May 2020; Accepted: 18 August 2020;
Published online: 2 November 2020

Related links
Key references using this protocol:
Branon, T. C. et al. *Nat. Biotechnol.* **36**, 880–887 (2018): https://www.nature.com/articles/nbt.4201
Cho, K. F. et al. *Proc. Natl Acad. Sci. USA* **117**, 12143–12154 (2020): https://www.pnas.org/content/117/22/12143

nature research

Corresponding author(s): Alice Y. Ting

Last updated by author(s): May 17, 2020

Reporting Summary

Nature Research wishes to improve the reproducibility of the work that we publish. This form provides structure for consistency and transparency in reporting. For further information on Nature Research policies, see our Editorial Policies and the Editorial Policy Checklist.

Statistics

For all statistical analyses, confirm that the following items are present in the figure legend, table legend, main text, or Methods section.

n/a	Confirmed	
☒	☐	The exact sample size (*n*) for each experimental group/condition, given as a discrete number and unit of measurement
☒	☐	A statement on whether measurements were taken from distinct samples or whether the same sample was measured repeatedly
☒	☐	The statistical test(s) used AND whether they are one- or two-sided *Only common tests should be described solely by name; describe more complex techniques in the Methods section.*
☒	☐	A description of all covariates tested
☒	☐	A description of any assumptions or corrections, such as tests of normality and adjustment for multiple comparisons
☒	☐	A full description of the statistical parameters including central tendency (e.g. means) or other basic estimates (e.g. regression coefficient) AND variation (e.g. standard deviation) or associated estimates of uncertainty (e.g. confidence intervals)
☒	☐	For null hypothesis testing, the test statistic (e.g. *F*, *t*, *r*) with confidence intervals, effect sizes, degrees of freedom and *P* value noted *Give P values as exact values whenever suitable.*
☒	☐	For Bayesian analysis, information on the choice of priors and Markov chain Monte Carlo settings
☒	☐	For hierarchical and complex designs, identification of the appropriate level for tests and full reporting of outcomes
☒	☐	Estimates of effect sizes (e.g. Cohen's *d*, Pearson's *r*), indicating how they were calculated

Our web collection on statistics for biologists contains articles on many of the points above.

Software and code

Policy information about availability of computer code

Data collection	UVP BioSpectrum Imaging System was used to acquire Western blots imaged with Clarity Western ECL Blotting Substrates (BioRad). Slidebook 6.0 was used to collect mammalian cell imaging data.
Data analysis	Slidebook 6.0 was used to analyze mammalian cell imaging data. ImageJ 1.50i was used to quantify Western blot data. MS data from TMT experiments was analyzed using Spectrum Mill MS Proteomics Workbench (Agilent Technologies).

For manuscripts utilizing custom algorithms or software that are central to the research but not yet described in published literature, software must be made available to editors and reviewers. We strongly encourage code deposition in a community repository (e.g. GitHub). See the Nature Research guidelines for submitting code & software for further information.

Data

Policy information about availability of data

All manuscripts must include a data availability statement. This statement should provide the following information, where applicable:

- Accession codes, unique identifiers, or web links for publicly available datasets
- A list of figures that have associated raw data
- A description of any restrictions on data availability

The data presented have been previously published; corresponding references are included and listed in Figure legends.

Field-specific reporting

Please select the one below that is the best fit for your research. If you are not sure, read the appropriate sections before making your selection.

☒ Life sciences ☐ Behavioural & social sciences ☐ Ecological, evolutionary & environmental sciences

For a reference copy of the document with all sections, see nature.com/documents/nr-reporting-summary-flat.pdf

Life sciences study design

All studies must disclose on these points even when the disclosure is negative.

Sample size	All mammalian cell imaging results presented were representative of at least 5 independent fields of view.
Data exclusions	There were no data exclusions.
Replication	The data presented have been previously published, the number of replicates for each experiment is detailed in the main original paper, Nature Biotechnology, 36, 880-887 (2018).
Randomization	No randomization methods were used because this was not applicable for our experiments.
Blinding	No blinding was used because this was not applicable for our experiments.

Reporting for specific materials, systems and methods

We require information from authors about some types of materials, experimental systems and methods used in many studies. Here, indicate whether each material, system or method listed is relevant to your study. If you are not sure if a list item applies to your research, read the appropriate section before selecting a response.

Materials & experimental systems

n/a	Involved in the study
☐	☒ Antibodies
☐	☒ Eukaryotic cell lines
☒	☐ Palaeontology and archaeology
☒	☐ Animals and other organisms
☒	☐ Human research participants
☒	☐ Clinical data
☒	☐ Dual use research of concern

Methods

n/a	Involved in the study
☒	☐ ChIP-seq
☒	☐ Flow cytometry
☒	☐ MRI-based neuroimaging

Antibodies

Antibodies used	antibody, vendor, catalog number: goat anti-mouse-HRP, BioRad, 170-6516; mouse anti-V5, Invitrogen, 46-0705; rabbit anti-calnexin, Santa Cruz Biotechnology, sc-11397; goat anti-mouse-AlexaFluor488, Invitrogen A-11029;goat anti-rabbit-AlexaFluor568, Invitrogen, A-11011
Validation	mouse anti-V5 (Invitrogen, 46-0705): several published immunofluorescence and Western blotting applications cited on website - https://www.thermofisher.com/antibody/product/V5-Tag-Antibody-Monoclonal/R960-25; rabbit anti-calnexin (Santa Cruz Biotechnology, sc-11397): several published applications cited on website - https://www.scbt.com/scbt/product/calnexin-antibody-h-70?requestFrom=search

Eukaryotic cell lines

Policy information about cell lines

Cell line source(s)	The source of the HEK 293T cell line was ATCC.
Authentication	The cell line (HEK293T) was not authenticated.
Mycoplasma contamination	The cells were not tested for mycoplasma contamination.
Commonly misidentified lines (See ICLAC register)	None. The only cell line used in this paper is HEK293T, which is not listed in the ICLAC database.